RESEARCH ARTICLE

Provenance and sediment routing of Neoproterozoic formations on the Varanger, Nordkinn, Rybachi and Sredni peninsulas, North Norway and Northwest Russia: a review

David Roberts* & Anna Siedlecka

Geological Survey of Norway, Post Box 6315 Sluppen, 7491 Trondheim, Norway.
**david.roberts@ngu.no*

Provenances and sediment routing of Neoproterozoic, mainly low-grade, sedimentary successions on four large peninsulas in Northeast Norway (Varanger and Nordkinn) and Northwest Russia (Rybachi and Sredni) have been assessed using a combination of abundant palaeocurrent data, lithological and petrographic features, heavy-mineral accumulations, a plentiful geochemical database and initial results of a detrital mineral isotopic study. The palaeocurrent data from both platformal and basinal domains on all four peninsulas show a remarkable consistency, with sediment dispersal directed largely towards the north (between NW and NE). Together with evidence from the other parameters, it has thus been possible to suggest various mafic to felsic terranes of Neoarchaean to Palaeoproterozoic age on the Fennoscandian Shield as likely source regions for the bulk of the detritus. An exception is provided by detrital zircon analyses from one prominent, NE-prograding, deltaic formation in the allochthonous basinal succession on Varanger Peninsula, which shows a profusion of Mesoproterozoic grains. An older submarine-fan formation in this same basin has been reported by others to show a comparable enrichment in Mesoproterozoic zircon grains. Taking into account a palinspastic restoration of this particular basinal terrane, the source of the deltaic detritus is likely to be concealed beneath the Caledonian nappes and present-day continental shelf, and could conceivably represent a northward extension of the Sveconorwegian/Grenvillian orogen, as has been suggested in recent literature. An alternative source could be that of a Tonian-emplaced, sandstone-dominated thrust sheet derived from the margin of Rodinia.

Roberts, D. and Siedlecka, A. (2012) Provenance and sediment routing of Neoproterozoic formations on the Varanger, Nordkinn, Rybachi and Sredni peninsulas, North Norway and Northwest Russia: a review. *Norges geologiske undersøkelse Bulletin*, **452**, 1-19.

Introduction

Studies of the provenance of sedimentary successions have traditionally focused on the lithologies, petrography and geochemistry of the rocks under investigation, in addition to sediment dispersal patterns indicated by palaeocurrent flow. Over the last two decades, however, increasing attention has been given to more sophisticated methods such as isotopic dating of detrital mineral species, notably zircon, coupled with Lu–Hf analysis, and geochemistry of a variety of heavy minerals (e.g., Morton and Hallsworth 1994, Morton et al. 1996, 2005, Cawood and Nemchin 2001, Kosler et al. 2002), all of which are conducive to refining palaeogeographic reconstructions and regional tectonic analysis.

In this contribution we consider the provenance and sediment routing systems of thick, passive-margin, sedimentary successions of mainly Neoproterozoic age occurring on four peninsulas flanking the Barents Sea in NE Finnmark, northern Norway, and in Northwest Russia (Figure 1). This particular region is especially interesting in that it records evidence of both Timanian and Caledonian orogenic deformation (Tschernyschev 1901, Schatsky 1952, Siedlecka 1975, Roberts 1995, 1996, Roberts and Siedlecka 2002, Herrevold et al. 2009). In addition, the low-grade rock successions of this region have also been the subject of several sedimentological studies, with a detailed record of palaeocurrent data for many of the formations, which is an ideal starting point for any reliable provenance investigation.

The earliest studies of parts of these Neoproterozoic successions aimed specifically at provenance evaluation are those of Siedlecka (1995), Sochava (1995), Sochava and Siedlecka (1997) and Siedlecka and Lyubtsov (1997). The paper by Sochava and Siedlecka (1997) is based on an assessment of the major-element geochemistry of over 400 samples of diverse sedimentary rocks from the Varanger, Rybachi and Sredni peninsulas. The work of Siedlecka and Lyubtsov (1997) was a pilot investigation involving heavy-mineral populations in sandstones, where the authors noted three disparate provenance areas on the shield based on the predominance of certain minerals in specific formations. Two studies have investigated the age spectrum of detrital zircons in formations on Varanger Peninsula (Kirkland et al 2008, Roberts et al. 2008, abstract). A study involving sedimentary geochemistry and preliminary detrital zircon analyses from parts of Varanger Peninsula has also been presented by Nicoll et al. (2009, abstract), some aspects of which are reproduced in Orlov et al. (2011). In addition to these provenance studies, there are several contributions dealing with palaeocurrent flow and sediment dispersal patterns in various formations occurring on the Rybachi, Sredni, Varanger and Nordkinn peninsulas, references for which are given below.

It should be mentioned at the outset that all directional data noted in this paper refer to present-day coordinates.

Geological setting

Varanger Peninsula

Neoproterozoic to Cambrian, fairly low-grade, sedimentary successions characterise the bedrock geology of Varanger Peninsula, which is divided into southwestern *platformal* (also called pericratonic) and northeastern *basinal* (passive margin) domains by the c. NW–SE-trending Trollfjorden–Komagelva Fault Zone (TKFZ) (Siedlecka and Roberts 1992) (Figure 2). The *c.* 4 km-thick platformal successions of the Tanafjorden–Varangerfjorden Region (TVR) are largely autochthonous to parautochthonous

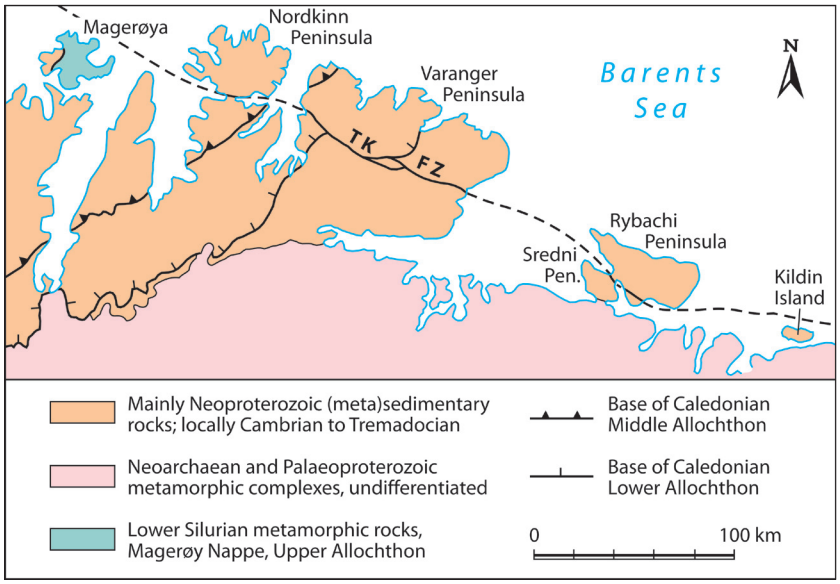

Figure 1. Outline map showing the locations of the Rybachi, Sredni, Varanger and Nordkinn peninsulas and Kildin Island. TKFZ – Trollfjorden–Komagelva Fault Zone.

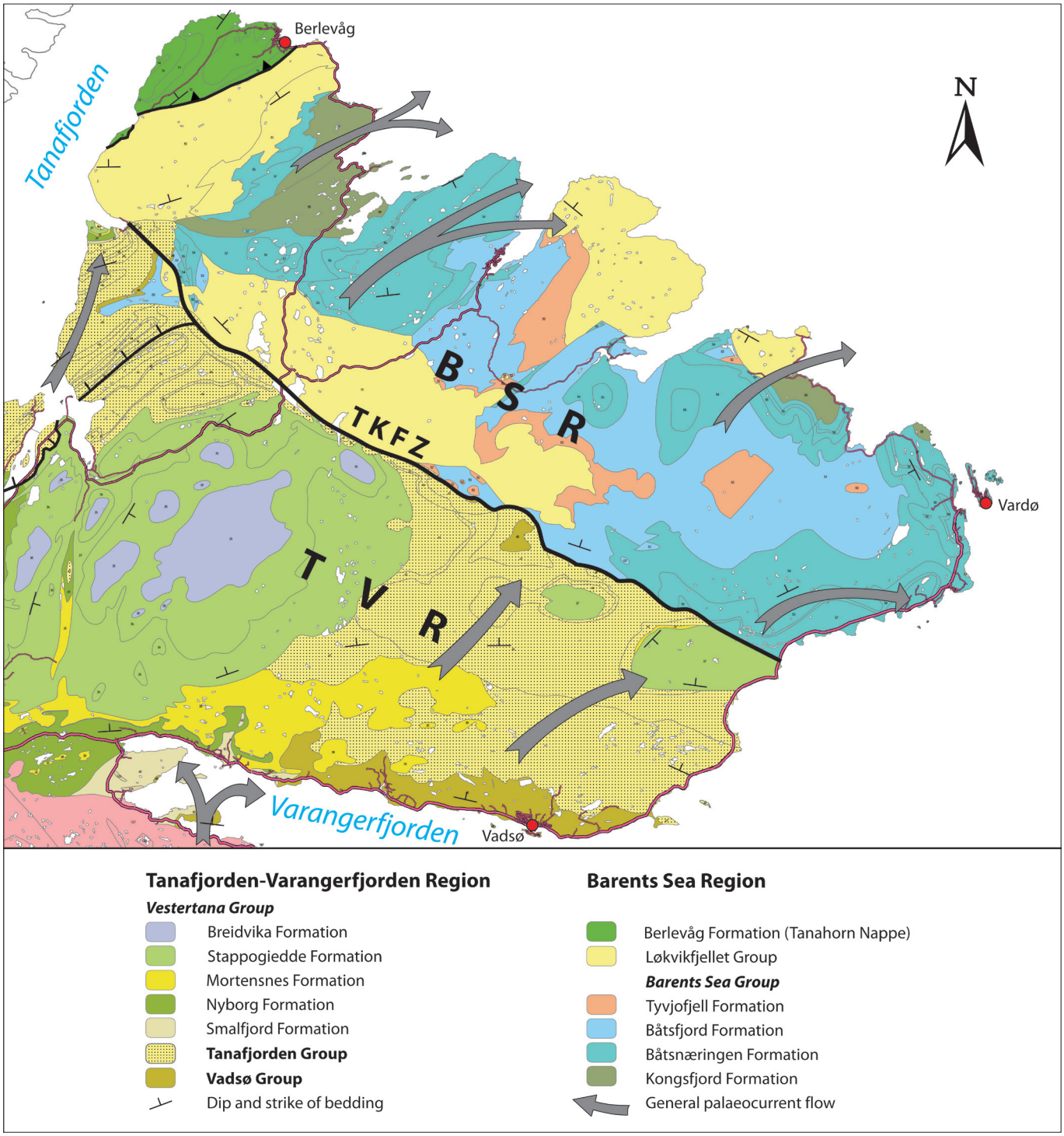

Figure 2. Simplified geological map of the Varanger Peninsula with the principal palaeocurrent flow indicated by the grey arrows. BSR – Barents Sea Region; TVR – Tanafjorden–Varangerfjorden Region; TKFZ – Trollfjorden–Komagelva Fault Zone. The base of the Tanahorn Nappe is marked by the thicker line with filled triangles. In the western part of the TVR, the thicker line with ticks marks the base of the Gaissa Nappe.

(diagenesis to anchizone grade) and comprise the fluvial (Figure 3a) to shallow-marine, Vadsø, Tanafjorden and Vestertana groups (Siedlecka 1985, Siedlecka and Roberts 1992). Rocks of the Vadsø Group, of inferred Tonian to early Cryogenian age, lie with angular unconformity upon Archaean granitic to granodioritic gneisses of the Fennoscandian Shield in the inner Varangerfjorden area (Banks et al. 1974, Rice et al. 2001). Three depositional sequences separated by important unconformities have been differentiated within the complete succession (Siedlecka et al. 1995a). The most significant break is the angular uncon-

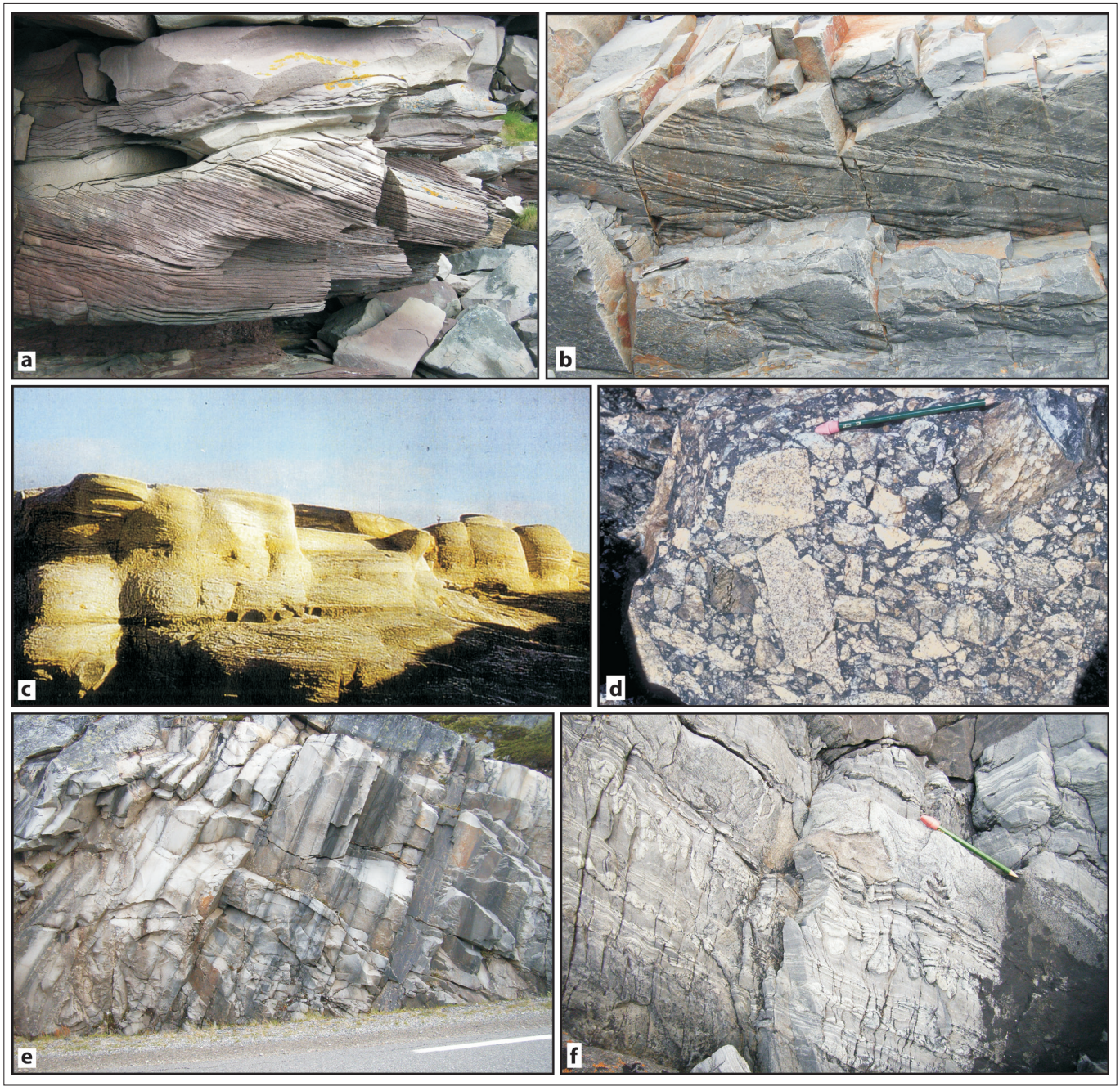

Figure 3. Field photos of selected lithologies; photos by D.R. except where stated. (a) Foreset bedding in cross-bedded sandstones of the Fugleberget Formation, Vadsø Group, Vadsø, Varangerfjorden; looking northeast. (b) Groove casts, frondescent marks and other sole marks on the bottom surfaces of two beds of greywacke, Kongsfjord Formation, Barents Sea Group, c. *5 km north of Kongsfjord; looking* c. *northwest. (c) Cross-bedded sandstones of the Zemlepakhtinskaya Formation, western coast of Sredni Peninsula. The dark layer is a leucoxene- and rutile-rich placer. Photo: Valery Lyubtsov. (d) Basal breccia/olistostrome of the Motovskaya Formation, Cape Vestnik, Rybachi Peninsula. The blocks and fragments consist mainly of Neoarchaean granitoid and gneissic rock types. (e) Medium- to thick-bedded and cross-bedded, feldspathic sandstones with thin silty layers,* c. *1 km east of Mehamn, Nordkinn Peninsula; looking* c. *northeast. (e) Thin-bedded and cleaved, alternating greywacke and silty mudstone with deformed load casts, current-rippled layers and possible dewatering structures,* c. *2 km south of Gamvik, Nordkinn Peninsula; looking north-northeast.*

formity between the Vadsø and likely Cryogenian Tanafjorden groups. The Vendian[1] to Cambrian, Vestertana Group includes two diamictites of glacial origin (the Smalfjord and Mortensnes formations) which are thought to correlate with the worldwide Marinoan and Gaskiers glacigenic events, respectively (Halverson et al. 2005, Rice et al. 2011). In the far northwest of this particular region (still southwest of the TKFZ), the Tanafjorden Group reappears in the Gaissa Nappe Complex (Figure 2), which is a part of the Lower Allochthon of Caledonide tectonostratigraphy. Just to the west on Digermul Peninsula, the succession in the Gaissa extends up into the Tremadocian (Reading 1965). Details of the subdivisions into Lower, Middle, Upper and Uppermost allochthons in the Scandinavian Caledonides are contained in Roberts and Gee (1985).

The basinal successions northeast of the TKFZ (Barents Sea Region, BSR) are allochthonous, mostly part of the Lower Allochthon, and of slightly higher metamorphic grade (epizone), and have been involved in modest, Caledonian (Early Ordovician), dextral strike-slip translation along the fault zone (Rice and Frank 2003); a figure in excess of 200 km has been suggested, based on palaeomagnetic data (Bylund 1994a, b). The successions comprise the 9 km-thick, mainly Tonian to Cryogenian, Barents Sea Group (deep-water submarine fan (Figure 3b) through deltaic to shallow-marine assemblages), the unconformably overlying, fluvial to shallow-marine, 5.7 km-thick Løkviksfjellet Group, of uncertain but probable Cryogenian age, and the slightly higher-grade rocks of the Berlevåg Formation of the Tanahorn Nappe, part of the Middle Allochthon (Figure 2) (Siedlecka 1972, Siedlecka and Edwards 1980, Pickering 1981, Siedlecka et al. 1989, Drinkwater et al. 1996), in the far northwest of the peninsula. An important link between the stratigraphic successions on either side of the TKFZ occurs in the Manjunnas area *c.* 10 km south of Trollfjorden. There, the highest formation in the Vadsø Group, the Ekkerøya Formation, lies unconformably above one of the formations of the Barents Sea Group (Rice 1994, Roberts and Karpuz 1995).

Taking Varanger Peninsula as a whole, there have been many sedimentological studies of diverse formations or complete groups (e.g., Banks et al. 1971, 1974, Laird 1972, Siedlecka 1972, 1978, Banks and Røe 1974, Røe 1975, 2003, Siedlecka and Edwards 1980, Pickering 1981, 1982a, b, 1983, Edwards 1984). The palaeocurrent record on this peninsula is thus one of the most comprehensive in the entire Caledonide orogen, a feature which augurs well for detrital zircon studies and interpretations. In general, palaeocurrent data are indicative of sediment transport from the southwestern to southern quadrant in both the platformal and the basinal domains, but there are some interesting diversions from this general rule with changing source regions between the different depositional sequences.

Rybachi and Sredni peninsulas

As on Varanger, the platformal and basinal domains are represented on the Rybachi and Sredni peninsulas on either side of a prolongation of the TKFZ, named the Sredni–Rybachi Fault Zone (SRFZ) (Roberts 1995) (Figure 4). The *c.* 2 km-thick, diagenesis-grade succession on Sredni Peninsula comprises the fluvial to shallow-marine Kildinskaya and Volokovaya groups (Figure 3c) of late Stenian to Cryogenian age based mainly on K–Ar dating of glauconite but also on one Pb–Pb date from a pebble of phosphorite (Negruta 1971, Siedlecka et al. 1995a). The succession correlates broadly with the Vadsø Group and parts of the Tanafjorden Group on southwestern Varanger Peninsula (Siedlecka et al. 1995a). In terms of sequence stratigraphy, four depositional sequences have been recognised in the Sredni succession. A basal, unconformable contact against Palaeoproterozoic granite is present in southernmost Sredni Peninsula. There is no record of diamictites or other rocks of Vendian/Ediacaran age on Sredni (Negrutsa 1971, Lyubtsov et al. 1989, Samuelsson 1997). Rocks of the Kildinskaya Group also occur c. 100 km farther east on Kildin Island (Siedlecka et al. 1995a). Palaeocurrent data are based on a variety of criteria such as cross bedding, ripple marks, graded bedding, sole marks and slump structures, and indicate sediment transport mainly from sources located to the southwest, south and southeast. Some differences, however, are seen between the different depositional sequences (Siedlecka et al. 1995a).

On Rybachi Peninsula, northeast of the SRFZ, a *c.* 4 km-thick, anchizone-grade succession (Rice and Roberts 1995) is representative of a basinal turbidite system overlain by upper slope deposits (Siedlecka et al. 1995b, Drinkwater et al. 1996). The two main units, the Einovskaya and Bargoutnaya groups (Figure 4), are considered to be of Tonian to Cryogenian age, and include a spectacular olistostrome-breccia (Figure 3d) near the base in the hangingwall to the SRFZ (Siedlecka et al. 1995b). The Rybachi turbidite system has been compared to the

[1] The term **Vendian**, introduced by Sokolov (1952) for the youngest period of the Neoproterozoic, has been, and still is, used in Russian and some Nordic geological literature. In 2006, the IUGS International Commission on Stratigraphy decreed that the name Vendian should be replaced formally by **Ediacaran**, named after the Ediacara Hills in Australia where the soft-bodied Ediacara fossils were first discovered. However, the time ranges of the Vendian and Ediacaran are not identical. Whilst both terminate upwards at the base of the Cambrian, the base of the Vendian is taken at the base of the Smalfjord (Marinoan) diamictite/tillite whereas the base of the Ediacaran is placed at the *top* of the Smalfjord Formation, just below a carbonate layer that caps the glacial deposit. Thus, the Ediacaran period is of shorter duration than the Vendian. In spite of losing its formality, the term Vendian is not invalid and can still be used as a legitimate chronostratigraphic unit. As it encompasses *both* the Smalfjord and the Mortensnes diamictites, within the Vestertana Group, we continue to use it here, rather than relegate the Smalfjord Formation to the Cryogenian.

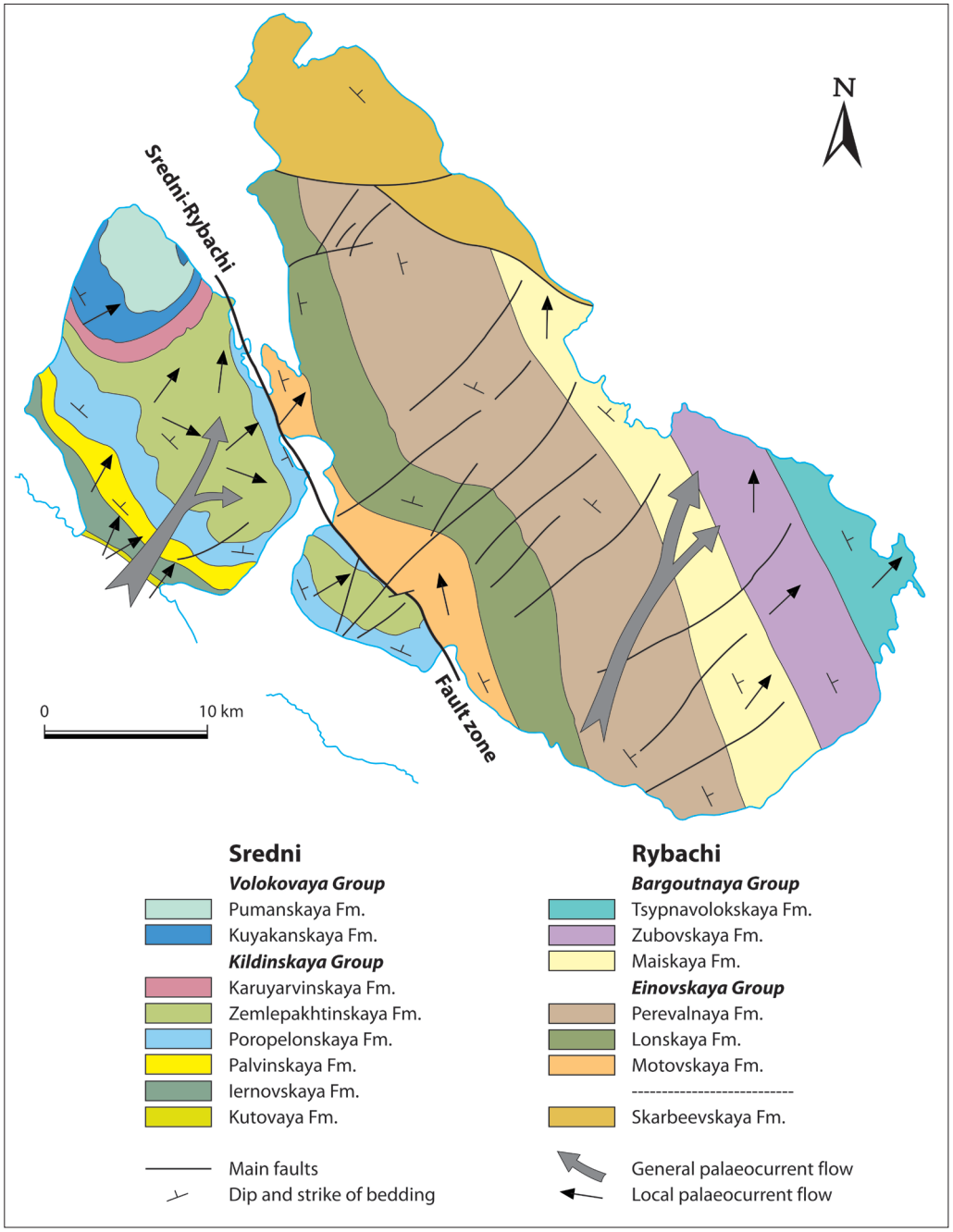

Figure 4. Geological map of the Rybachi and Sredni peninsulas, Northwest Russia, showing the general palaeocurrent flow and also local, formation-scale, flow vectors (taken from figures and information given in Negrutsa (1971) and Siedlecka et al. (1995a and b) supplemented by a few observations during fieldwork in 1990, 91 and 93).

Kongsfjord submarine fan in the basinal domain of Varanger Peninsula (Siedlecka et al. 1995b, Drinkwater et al. 1996), both developing across the shelf-slope break between the platformal and basinal domains marked by the major TKFZ/SRFZ fault system.

Nordkinn Peninsula

The metasedimentary rocks on the Nordkinn Peninsula (Figure 5) constitute a lower part of the Kalak Nappe Complex, which is generally assigned to the Middle Allochthon (Roberts and Gee 1985, Rice and Frank 2003, Gee et al. 2008). The greenschist-facies lithologies form a coherent succession and range from thick-bedded arkosic sandstones through interbedded sandstones and phyllites (Figure 3e) to more pelitic units containing porphyroblasts of biotite and garnet (Rice and Roberts 1988). In addition, orthoquartzite units >200 m in thickness occur in western and some eastern parts of Nordkinn. Because of lithological repetitions and sedimentary facies changes it has not yet been possible to establish a formal lithostratigraphy on this peninsula. Based on correlations with similar successions occurring immediately to the south and southwest, the siliciclastic rocks of Nordkinn are probably of latest Mesoproterozoic (Stenian) to Early Neoproterozoic (Tonian) age (Kirkland et al. 2007). This

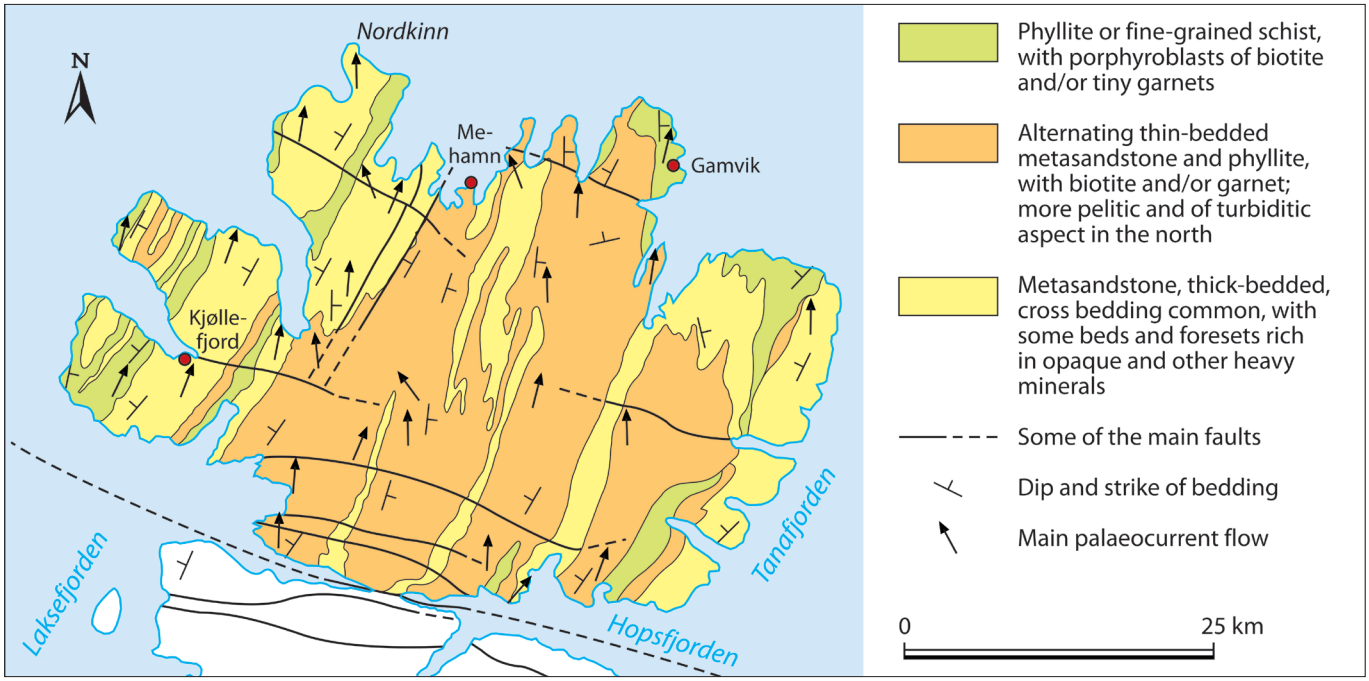

Figure 5. Simplified geological map of Nordkinn Peninsula showing palaeocurrent flow as measured in cross-bedded sandstones (corrected for dip of bedding and fold plunge).

age assignment relies on the detrital zircon U–Pb dating of one sample from Sværholt Peninsula by the aforementioned authors, and should therefore be considered as preliminary.

Cross-bedding is a common feature of the thicker sandstones with basal layers and foreset strata showing striking enrichments in a variety of heavy minerals, producing a distinctive black-and-white striping of the rock (Roberts 2007, figure 3). Many such cross-beds show penecontemporaneous deformation of the foresets (Roberts and Andersen 1985), a feature which has also been described from sandstones in the area directly south of Nordkinn Peninsula (Williams 1974) and in the subjacent Laksefjord Nappe Complex (Chapman 1980). In the more thinly interbedded and partly pelitic units, there are many examples of graded bedding, ball-and-pillow structures and sole marks (Figure 3f), typical of turbidites, together with chaotic sediment slide and slump structures, especially in northern areas. Considering the Nordkinn Peninsula as a whole, it appears that there is a gradual facies change from south to north from a dominantly fluvial to prodelta regime to a marine, turbidite association, reflecting a palaeobasin deepening roughly northwards (Roberts 2007).

Precambrian basement

In the Varangerfjorden–Kola region, the crystalline basement forming the substrate to the autochthonous formations of the Vadsø and Kildinskaya groups is dominated by Archaean complexes which range in age from 2.9 to 2.5 Ga (Levchenkov et al. 1995, Koistinen et al. 2001) and form part of the Murmansk Terrane. Some 50–200 km farther southwest, across NW–SE-trending suture zones, follow the Neoarchaean Inari Terrane and the 2.0–1.9 Ga Lapland Granulite Belt. Rocks in both these terranes were variably reworked during the diachronous, 1.95–1.87 Ga, Lapland–Kola orogeny (Daly et al. 2001, 2006). This collisional event is regarded as an early phase of the composite, Palaeoproterozoic, Svecofennian orogeny (1.95–1.77 Ga), the rocks and structures of which occur extensively farther southwest in northern Finland, Norway and Sweden (Gaál and Gorbatschev 1987, Korja et al. 2006, Lahtinen et al. 2008). Finally, rocks of suspected Mesoproterozoic age are inferred to be present farther west beneath the Caledonian nappes (Roberts 2007, Kirkland et al. 2011, Lorenz et al. 2012).

Basement to the basinal successions of the northeastern Varanger and Rybachi peninsulas northeast of the TKFZ/SRFZ is nowhere exposed. However, accepting that this major fault functioned as an extensional, shelf-edge structure during Neoproterozoic and even Late Mesoproterozoic time, then it is highly likely that the basin is underlain by Archaean complexes akin to those exposed in the Murmansk Terrane.

Main structural features of the Neoproterozoic successions

Rocks of the Parautochthon and Lower and Middle Allochthons on the Varanger and Nordkinn peninsulas are part of the Caledonide fold-and-thrust belt and were clearly involved in Caledonian deformation. Fold axes, an associated schistosity and thrust-faults trend approximately NE–SW ± 20° (Roberts 1972, Siedlecki 1980, Rice et al. 1989, Herrevold et al. 2009). Geochronological evidence is suggesting that the main structures

and schistosity in northwestern Varanger Peninsula date to Early Ordovician time, with a more brittle event in the Mid to Late Silurian (Rice and Frank 2003), possibly extending into the Early Devonian (Kirkland et al. 2008). The main, dextral, strike-slip translation along the TKFZ occurred during Early Ordovician time (Rice and Frank 2003). Only limited data are so far available for the Nordkinn Peninsula. A sample of biotite phyllite subjected to laser-ablation Ar–Ar dating yielded an age of c. 500 Ma (Kirkland et al. 2008), interpreted by these authors as dating the greenschist-facies tectonometamorphic event as well as the main thrust emplacement of the Kalak Nappe Complex.

On the Rybachi and Sredni peninsulas, folds and an associated, steep, slaty cleavage trend NW–SE and are considered to relate to the Timanian orogeny, the type area for which is farther southeast in the Timans of the Komi Republic (Olavyanishnikov et al. 2000, Roberts and Siedlecka 2002, Gee and Pease 2004). The main phase of this orogenic event dates to approximately 600–560 Ma, i.e., of Vendian/Ediacaran age (Olovyanishnikov et al. 2000, Larionov et al. 2004, Roberts and Olovyanishnikov 2004), but orogenesis extended up into Early Cambrian time in some peripheral areas (e.g., Beckholmen and Glodny 2004, Pease and Scott 2009, Orlov et al. 2011). Comparable NW–SE- to NNW–SSE-trending folds and associated axial-planar cleavage occur in northeasternmost Varanger Peninsula (Roberts 1995, 1996, Herrevold et al. 2009), and the NW–SE trend is also registered on the seabed in outer Varangerfjorden (Roberts et al. 2011) as well as in aeromagnetic data (Gernigon et al. 2008, Brönner et al. 2009).

Provenance and sediment routing indicators

In this section we present the various evidence that has a direct bearing on the provenance of the Neoproterozoic successions occurring on the different peninsulas, and also on the sediment dispersal patterns or routing systems of these deposits. As this is a summary of the data and observations, we cite the many publications where readers can access the full details in their particular area of interest. For each indicator, we describe the peninsular areas from east to west.

Palaeocurrent data

In the autochthonous succession of *Sredni Peninsula*, palaeocurrent data derive mainly from cross-bed foresets in several sandstone formations recorded by Negrutsa (1971) and summarised in figure 4 in Siedlecka et al. (1995a). In general, a fairly unimodal flow from a SW to SE source characterises the succession as a whole (Figure 4), indicative of derivation of the sediment probably from the nearby Neoarchaean to Palaeoproterozoic complexes of the Fennoscandian Shield. However, there are noticeable differences of flow vector between the four depositional sequences (Siedlecka et al. 1995a), which may relate to tectonic activity and changing source areas in the hinterland or to fluctuating coastline configuration.

Information on current flow during deposition of sandstone formations on *Rybachi Peninsula* is minimal, but again a sediment dispersal towards a northerly point has been indicated by measurements from near the base of the Einovskaya Group (flow towards NW) and in the Bargoutnaya Group (flow between N and NE) (Negrutsa 1971, in Siedlecka et al. 1995b). The entire Rybachi submarine-fan system is considered to have accumulated by basinward progradation away from the shelf-slope break (Siedlecka et al. 1995b, figure 20), with a slight clockwise swing which may have been associated with downslope currents turning into the axial elongation of the deep-marine basin.

On *Varanger Peninsula*, the autochthonous to parautochthonous Vadsø and Tanafjorden groups south of the TKFZ have yielded a large amount of data on palaeocurrent flow by many authors (Reading and Walker 1966, Banks 1971, Banks et al. 1971, 1974, Siedlecka and Siedlecki 1971, Banks and Røe 1974, Hobday 1974, Røe 1970, 1975, Edwards 1984). In this shallow pericratonic basin, with 8 or 9 transgressive/regressive cycles and with intertidal environments recognised in several formations, the directional variance of the currents is comparatively high, yet overall we again see a predominance of sediment dispersal towards the NE to NW quadrant (Siedlecka et al. 1995a) (Figure 2). A more complex palaeogeographical scenario marked the start of Vendian time and deposition of the Vestertana Group, following tectonic uplift and erosion, with the glaciogenic diamictite formations showing ice-sheet advances and sediment infill into a shallow epicontinental basin from both the south and the north (Edwards 1984). A southwesterly sediment source characterised the inter-glacial Nyborg Formation (Banks et al. 1971, Edwards 1984). Interestingly, the immediate postglacial era (Stappogiedde Formation) records a major input of detritus from a northeasterly source, based on the sedimentological studies of Banks et al. (1971), a feature which has been considered by Roberts and Siedlecka (2002) to relate to erosion of the rising deformation front of the Timanide orogen and deposition in a small foreland basin. In this regard, a burial diagenesis age of *c.* 560 Ma for Stappogiedde shales (Gorokhov et al. 2001) is in accord with this interpretation. Farther to the southeast, in the White Sea area of Russia, the Vendian succession of the Mezen Basin has also been interpreted as relating to Timanian orogenesis (e.g., Schatsky 1952, Grazhdankin 2004), with the sediment input into the foreland basin sourced from the northeast.

The geology of the BSR, northeast of the TKFZ, is dominated by the Barents Sea Group with its prominent, deep-water, Kongsfjord submarine fan (Siedlecka 1972, 1985, Pickering 1981, 1982a, b, 1983, 1985) which records current

flow towards NE–E, away from the shelf edge (Figure 2). This was superseded by deltaic to shallow-marine environments, with the deltaic sediments showing a general ENE progradation (Siedlecka and Edwards 1980, Pickering 1982a, Siedlecka et al. 1989). Overlying formations of the shallow-marine to locally fluvial Løkviksfjellet Group show a fairly unimodal pattern of sediment dispersal and current flow directed towards the NNE to ENE quadrant (Laird 1972, Levell 1978). It is appropriate here to note that although the Løkviksfjellet Group has been loosely correlated chronostratigraphically with the largely Vendian, Vestertana Group succession of the TVR (Vidal and Siedlecka 1983), the poor acritarch taxa recovered from this group by these authors are in no way time-diagnostic. Thus, the precise age of the Løkviksfjellet Group is unknown. The character and chemistry of the deposits (see below) and the palaeocurrent evidence, however, do not accord with features typical of the Vestertana Group; and there is no evidence of a northeasterly source for any of the sediment input. Moreover, Kirkland et al. (2008) have noted that a Sm–Nd model age for a psammite from the Løkviksfjellet Group is similar to model ages from metasedimentary rocks of the Kalak Nappe Complex. The various evidence therefore points toward a pre-Vendian and most likely Cryogenian age for this group.

Structurally overlying the Løkviksfjellet Group, the Berlevåg Formation of the Tanahorn Nappe (interpreted as part of the Middle Allochthon) has not provided any reliable palaeocurrent data, but there are clear facies changes indicative of finer-grained, more distal elements towards the north where diverse sole marks and flute casts are quite common on the bottom surfaces of greywacke beds.

Palaeocurrent data from the thick, late Stenian to Tonian, sandstone units on *Nordkinn Peninsula* are based on abundant cross bedding, ripple marks and parting lineations and document a fairly unimodal flow towards NW–NNW with a minor azimuth directed NNE (Roberts 2007) (Figure 5). Coupled with the regional facies change noted earlier, this accords with the presence of a palaeobasin situated towards the 'north' at the time of sediment accumulation. Since the rocks on Nordkinn are allochthonous, the fluvial system and distal basin would have been located at some unknown distance to the northwest prior to Caledonian thrusting (cf. Gayer et al. 1987).

Lithological indicators

Lithology and petrography of sedimentary rocks can provide important clues regarding provenance, particularly where blocks, boulders and small rock fragments in breccias and conglomerates can be identified with relative confidence. On *Sredni Peninsula*, there is little documented evidence in this regard, although conglomerates at the bases of the four depositional sequences are reported to contain extrabasinal pebbles of granitic rock types derived from southerly sources (Negrutsa 1971, Siedlecka et al. 1995a). Clasts of phosphorite in a 30 m-thick bed at the base of the Volokovaya Group have been interpreted by Negruta (1971) and Negrutsa et al. (1995) to derive from bedded phosphorite horizons in the subjacent Kildinskaya Group (Negrutsa 1971, Negrutsa et al. 1995).

Rybachi Peninsula, on the other hand, exposes an olistostrome-breccia at the base of the Einovskaya Group (Motovskaya Formation) containing angular blocks and fragments of diverse granitoid rocks and gneisses (Siedlecka et al. 1995b, Lyubtsov et al. 1999) (Figure 3d). According to Negrutsa (1971), one exotic block of granite measures over 100 m across. The fragmentary clast material in the breccia is clearly of local derivation, probably ripped away from the Neoarchaean crystalline basement (Levchenkov et al. 1995, Koistinen et al. 2001) of the Murmansk Terrane below the edge of the Sredni platform in the footwall of the SRFZ. Other conglomerates higher up in the Rybachi succession are also polymict and contain a variety of granitic and gneissic clasts, interpreted to be derived from known Neoarchaean and Palaeoproterozoic terranes in the shield area to the south (Siedlecka et al. 1995b). Lenses of a well-sorted boulder conglomerate are present in one formation, with rounded boulders of granite (Lyubtsov et al. 1999).

In southern *Varanger Peninsula* and inner Varangerfjorden, the autochthonous succession lies with an angular unconformity upon Neoarchaean granitic and tonalitic gneisses, and clasts within the braided fluvial and prodelta sandstones and conglomerates signify derivation from both external and intraformational sources (Banks et al. 1974, Rice et al. 2001, Røe 2003) (Figure 3a). In several places, the basal Smalfjord Formation diamictite of the Vendian/Ediacaran Vestertana Group lies directly upon the crystalline Archaean basement (Føyn & Siedlecki 1980, Edwards 1984). Clasts in this formation include both granitic gneisses of local derivation (from the south) and more common dolomitic and arenaceous rocks from the Tanafjorden Group (from diverse sources) (Edwards et al. 1973, Edwards 1984, Rice et al. 2011).

The succession in northern Varanger Peninsula provides comparatively few clues regarding the actual provenance of the original sediments, but rock fragments and small clasts in the Kongsfjord fan have been interpreted as deriving mostly from felsic plutonic and volcanic rocks as well as gneissic complexes (Siedlecka 1972, Pickering 1981). As both the submarine fan and the succeeding Båtsnæringen Formation delta prograded northeastwards, this is again suggestive of a sediment source on the shield. As the delta was originally located farther to the northwest (p. 13), then the source rock terrane (prior to dextral translation along the TKFZ) is likely to have been one now concealed beneath the Caledonian nappes (Roberts 2007, Lorenz et al. 2012). The Båtsnæringen Formation also contains phosphorite fragments, considered to be redeposited from bedded phosphorites akin to those in the platformal succession on Sredni Peninsula (Negrutsa et al. 1995). The unconformably overlying, feldspathic sandstones of the Løkviksfjellet Group

show a marked change towards textural and mineralogical maturity. This points to sediment transport from a completely different, but southwesterly, source region following an event of uplift, tilting and erosion prior to deposition of the Sandfjorden Formation.

On *Nordkinn Peninsula*, no detailed petrographic study of the sandstones and small-clast conglomerates has yet been carried out. Accordingly, at this stage, lithology alone cannot contribute to the discussion of sediment provenance.

Heavy-mineral accumulations

Assemblages of heavy minerals are considered to be important and sensitive indicators of sediment provenance (Morton and Hallsworth 1994, 1999), even though the original provenance signal may have been disturbed, to some extent, by processes such as weathering, diagenesis and hydrodynamics. Studies of such mineral accumulations and individual mineral chemistry have proved valuable in linking sediment to source, also in present-day rivers in Norway (Morton et al. 2004).

On the *Sredni* and *Rybachi* peninsulas, concentrations of heavy minerals have been reported from the Zemlepakhtinskaya Formation of the Volokovaya Group on Sredni, where palaeoplacer deposits occur at two stratigraphic levels in this same formation (Negrutsa 1971, Siedlecka et al. 1995a). These consist mainly of titanomagnetite and zircon concentrates, but dark-grey to black sandstones with high contents of leucoxene and rutile have also been reported (Lyubtsov et al. 1999) (Figure 3c). Several formations of the Kildinskaya Group on Kildin Island also contain layers rich in zircon, rutile, apatite, titanite, tourmaline and opaque minerals (Lyubtsov et al. 1999) and small placers of titanomagnetite have been reported (Sochava 1995).

On *Varanger Peninsula*, a pilot study of heavy-mineral assemblages in thirteen different formations in both the autochthonous and the allochthonous successions has been reported by Siedlecka and Lyubtsov (1997), aiming specifically to provide evidence on provenance. The mineral concentrations studied were those of zircon, tourmaline, garnet, rutile and apatite (Figure 6) with >100 counts per sample. The results showed that at least three provenance areas in the crystalline shield contributed to the Neoproterozoic sedimentary successions; one, with a dominance of zircon in the heavy fraction and inferred by Siedlecka and Lyubtsov (1997) to derive from granites and granodiorites, is fairly widespread (Figure 6); a second, wherein tourmaline predominates, probably sourced from granites, gneisses and possibly pegmatites, is restricted to the Tanafjorden Group (Figure 6, lower part); and a third, with common garnet, which provided material to the interglacial Nyborg Formation. Whereas the zircon and tourmaline are likely to derive from Neoarchaean rocks, the garnet source (to the southwest, from palaeocurrent data) was quite possibly within the Palaeoproterozoic Lapland Granulite Belt (Siedlecka and Lyubtsov 1997). As well as these features, there are also fairly marked differences in heavy mineral content between samples in the two separate regions of Varanger Peninsula (Figure 6).

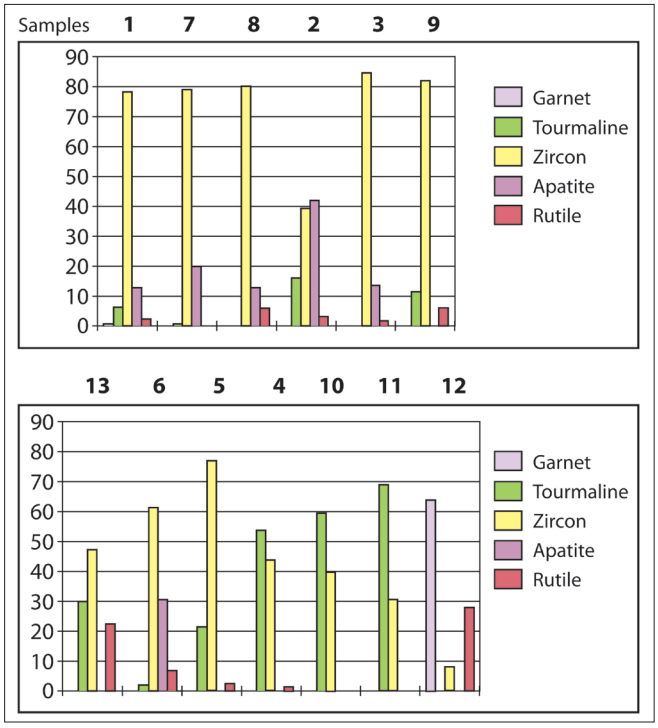

Figure 6. Heavy-mineral distributions in samples of sandstones from thirteen formations on Varanger Peninsula. Lower panel – formations in the platformal Tanafjorden–Varangerfjorden Region; upper panel – formations in the basinal Barents Sea Region. The formations are as follows (lower panel first): 13 – Veidnesbotn: 6 – Fugleberget: 5 – Golneselva: 4 – Dakkovarre: 10 – Gamasfjellet: 11 – Hanglečærro: 12 – Nyborg: 1, 7 & 8 – Kongsfjord: 2 & 3 – Båtsnæringen: 9 – Sandfjorden. The figure is modified from Siedlecka and Lyubtsov (1997, figure 3).

The feldspathic metasandstones of the Kalak Nappe Complex on *Nordkinn Peninsula* (Figure 3e) are in many places characterised by heavy-mineral accumulations, marked by dark-grey to black intercalations rich in titanomagnetite and/or magnetite. These occur either as thin beds (up to 2 cm), lensoid deposits or as enrichments in foreset strata in cross-bedded units (Roberts and Andersen 1985, Roberts 2007, figure 3). Closer inspection has revealed the common presence of titanite, rutile, apatite and monazite in these layers and foresets, with accessory garnet and tourmaline. Coupled with the palaeocurrent data, indicative of a broadly north- to northwestward sediment dispersal, we consider that these heavy-mineral concentrates are likely to have derived from the diverse basement terranes on the Fennoscandian Shield.

Geochemistry

The geochemistry of diverse lithologies in the Neoproterozoic successions on the *Sredni*, *Rybachi* and *Varanger peninsulas* was investigated in great detail in the 1990s, though at that time based wholly on major-element analyses (Siedlecka 1995,

Sochava 1995, Sochava and Siedlecka 1997). Nevertheless, no fewer than 461 samples were analysed by XRF, 231 from Sredni and Rybachi and 230 from Varanger, and the complete analytical data were evaluated by classification diagrams and cluster dendrograms (Sochava and Siedlecka 1997).

A principal result of this study is that there is a clear compositional distinction between the platformal and basinal domains on either side of the major TKFZ/SRFZ, with K_2O > Na_2O south of the fault whereas high contents of Na_2O, MgO, FeO and CaO predominate in rocks of the turbiditic to deltaic, basinal successions. A similar conclusion was reached by Nicoll et al. (2009). Compositions of the basinal successions were interpreted by Sochava and Siedlecka (1997) as relating to a tectonically active source region with likely derivation from the mafic to intermediate rocks of the Palaeoproterozoic Pechenga Greenstone Belt. Sources of unknown age, but possibly Mesoproterozoic, farther west in the basement beneath the Caledonian nappes, but not exposed today, are also likely to have been involved.

The Sandfjorden Formation of the Løkviksfjellet Group shows a distinctive geochemical signature that differs from formations of the Barents Sea Group in having higher K_2O and SiO_2 contents (Sochava and Siedlecka 1997). This is indicative of derivation from a different source area to the south following the tectonic event that gave rise to the uplift, tilting and unconformity at the base of the Løkviksfjellet Group.

The geochemistry of shales showed interesting changes, even within the same formation, indicative of a changing provenance and/or climatic variations. Sandstones and siltstones of the Ediacaran Stappogiedde Formation show compositions which differ quite markedly from those of underlying formations and, along with the evidence of changing palaeocurrent flow, may relate to derivation from the rising topographic front of the Timanian orogenic belt.

Rare-earth element (REE) analyses exist from 24 shales from different formations on Rybachi Peninsula (K.T. Pickering, unpublished data). The REE patterns in these particular shales are quite variable and are thus indicative of rapidly changing sources and river catchments for the sediment influx onto the platform and its redistribution via deltas and submarine fans into the basinal regime.

For *Nordkinn Peninsula*, there is as yet no published documentation on the geochemistry of rocks in the Kalak Nappe Complex.

Isotopic studies on detrital minerals

Until recently, the only published isotopic studies on detrital minerals in rocks from the investigated peninsulas were those of Gorokhov et al. (2001, 2002) and Kirkland et al. (2008). An additional study, on six formations from Varanger Peninsula, has just become known to us (Orlov et al. 2011; a translation of an original Russian text), and provides important information regarding the provenance of these sandstones.

Rb–Sr dating studies on illite from shales on *Sredni* and *Varanger* (Gorokhov et al. 2001, 2002) have shown that the coarser grain-size, 2M1, illite polytype is clearly detrital with minimum ages of 830 Ma (Sredni) and *c.* 930 Ma (Varanger), and derives from the source area or areas of the sediments, which are inferred to have lain somewhere to the south of the sites of deposition of these autochthonous formations. Other, very low-grade, authigenic, illite polytypes relate to burial diagenesis and other events in Ediacaran and Siluro–Devonian time (Gorokhov et al. 2001, 2002).

Preliminary results of a provenance study employing U–Pb (LA–ICP–MS) analyses of detrital zircons from four formations from *Varanger Peninsula* were presented by Roberts et al. (2008) and Slagstad et al. (2011). For the interglacial Nyborg Formation of the Vestertana Group, one population group dominates the probability plot at 2.0–1.85 Ga with a minor spread between 3.0 and 2.5 Ga (Figure 7b). No Mesoproterozoic zircon grains were analysed. This frequency plot contrasts markedly with that of the deltaic Båtsnæringen Formation, from north of the TKFZ, which shows a multimodal spread from *c.* 2.1 to 1.0 Ga with spikes at 1.80–1.65, 1.45–1.40 and 1.25–1.0 Ga (Figure 7a). There are also subsidiary peaks at 2.1–2.0 and 2.9–2.6 Ga. Zircons from this formation vary greatly from short prismatic grains to well rounded, elongate forms (B.Davidsen and T.Slagstad, unpublished data). Zircons from the Sandfjorden Formation show two groups at 2.0–1.75 and 2.9–2.6 Ga with a few grains in the range 1.6–1.0 Ga (Figure 7c). For the Berlevåg Formation of the Tanahorn Nappe, the probability plot depicts one main group at 1.9–1.7 and a minor spread at 2.9–2.6 Ga (Figure 7d). A comparable plot for the Berlevåg Formation has been presented by Kirkland et al. (2008) who also reported an oldest zircon grain of 3136 ± 13 Ma.

In general, the detrital zircon data are thus indicative of derivation from Archaean to Palaeoproterozoic basement terranes that lay roughly to the south of where the Neoproterozoic formations occur today. The Cryogenian Båtsnæringen Formation is the prime exception here, containing much Mesoproterozoic detritus from a source not exposed in northern Fennoscandia at the present time but possibly concealed beneath the Caledonian nappes and adjacent continental shelf (Roberts 2007, Be'eri et al. 2011, Lorenz et al. 2012). Considering the pre-Caledonian location of the Barents Sea Region (see discussion), this is not an unreasonable suggestion. However, accepting the proposition that some initial thrusting of the Kalak sedimentary rocks onto older basement is likely to have occurred in Tonian time, associated with a late-Sveconorwegian event (Kirkland et al. 2006), then the Mesoproterozoic zircons of the Båtsnæringen delta, particularly those that are well rounded and most likely recycled, may have been sourced from this early allochthon.

The work of Orlov et al. (2011) depicts probability plots for four formations from the pericratonic domain on Varanger and two from the basinal Barents Sea Group. Their plot of detrital

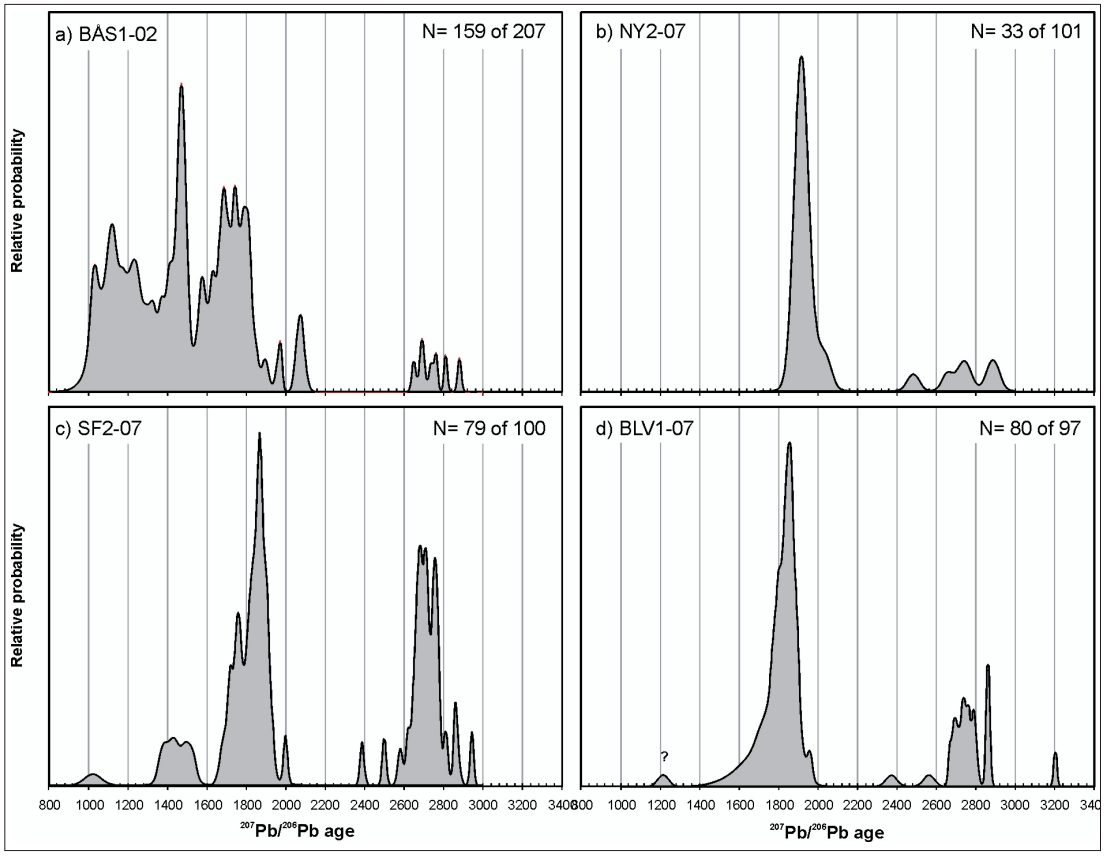

Figure 7. Probability density versus age (common-Pb corrected, $^{207}Pb/^{206}Pb$) plots of detrital zircons from very low-grade metasandstones of the (a) Båsnæringen Formation, Barents Sea Group, (b) Nyborg Formation, Vestertana Group and (c) Sandfjorden Formation, Løkviksfjellet Group; and (d) greenschist-facies metasandstone of the Berlevåg Formation, Tanahorn Nappe. The probability density plots include ages with <10% discordance. The number of grains that are <10% discordant and the total number of analysed grains are indicated. The figure is modified from one depicted in Roberts et al. (2008). The zircons were analysed by Børre Davidsen and Trond Slagstad at NGU, Trondheim. Precise sample locations can be obtained from the first author upon request.

zircon analyses from the Båtsnæringen Formation is comparable to ours (in Figure 7a); and interestingly, a sample from the Kongsfjord Formation shows a very similar pattern, with a dominance of Mesoproterozoic and Late Palaeoproterozoic grains. Samples from the Andersby (Vadsø Group), Dakkovarre (Tanafjord Group) and Mortensnes (Vestertana Group) formations also show a series of peaks between 2.0 and 1.0 Ga. It therefore seems clear that a Mesoproterozoic source (or possibly successions containing recycled Mesoproterozoic zircons) was available for erosion and fluvial and marine-current dispersal during the deposition of these platformal Tonian–Cryogenian successions on southern Varanger Peninsula. Moreover, the Mesoproterozoic source, or sources, is even more prominent in the case of the allochthonous, basinal, Båtsnæringen and Kongsfjord formations.

As yet there are no detrital zircon data from rocks on the *Nordkinn Peninsula*. However, along strike to the southwest, zircon analytical data have been reported by Kirkland et al. (2007) from two samples of psammite and one of pelite from the lower thrust sheets of the Kalak Nappe Complex, with the oldest zircon grains in the range c. 2.88 to 2.67 Ga. These various data were interpreted by Kirkland et al. (2007) to suggest that sedimentation of these rocks was confined to the period c. 1030 to 980 Ma, Late Stenian to Early Tonian. The upper constraint for deposition was based on a U–Pb zircon age of 981 ± 7 Ma for a strongly foliated granite in a thin thrust slice within the lithostratigraphy in the eastern part of the Porsanger Peninsula (Kirkland et al. 2006).

Discussion

To produce a truly comprehensive picture of provenance and sediment dispersal patterns of depositional systems in any region requires the interpretation of a variety of sedimentological, lithological, geochemical and isotopic age data. On their own, these parameters provide just one facet of the sediment source terrane puzzle, but in combination they constitute a powerful tool in assessing the likely source regions, their location, composition and age, and sediment dispersal pathways of the successions under scrutiny.

In the case of the lithological successions considered here we are fortunate in having a robust sedimentological database founded on detailed geological maps, both of which have led to diverse studies in a variety of disciplines. Taking the platformal or pericratonic domain on both Sredni and Varanger, sediment source areas clearly lay mainly to the south but there are significant variations in palaeocurrent flow directed between northwest and northeast which correlate to some extent with specific depositional sequences floored by important unconformities. These in turn relate to changes in erosion level,

relief rejuvenation at the source or likely ephemeral ponding within the catchments, a response to repetitive epeirogenic events and tilting that affected the shield throughout Neoproterozoic time.

Confirmation of these diachronous changes in provenance are seen in the geochemical and heavy-mineral data, notably from granite- and zircon-dominated source regions to areas of the shield underlain by garnetiferous metamorphic rocks, e.g., the Lapland Granulite belt. As yet we have limited information from detrital mineral isotopic data but source ages are mainly Late Palaeoproterozoic and Neoarchaean, conforming to the present-day exposed terranes of the Fennoscandian Shield (Levchenkov et al. 1995, Koistinen et al. 2001). However, the work of Orlov et al. (2011) has signified that Mesoproterozoic source terranes, or successions containing recycled Mesoproterozoic grains, were also available to erosion during Tonian–Cryogenian and Early Vendian time. Departures from the otherwise consistent southerly source story appear only in Vendian time on Varanger Peninsula where diamictites of the Vestertana Group show local derivation from the north. More significant is the evidence of a northeasterly source for sediments deposited in the immediate post-glacial era (Stappogiedde Formation), effectively implying the presence at that time of a small foreland basin ahead of the rising Timanian deformation front (Gorokhov et al. 2001). This accords with the evidence of a foreland basin (Mezen Basin) situated immediately southwest of the Timans (Grazhdankin 2004).

Assessment of the provenance or provenances of the basinal successions on Rybachi Peninsula and on the Varanger Peninsula northeast of the TKFZ has to take into account their dextral translation of more than 200 km during the Caledonian cycle. Thus, the Timanian-deformed Rybachi succession, comprising an early shelf-edge olistostrome and a subsequent greywacke-dominated submarine fan, probably accumulated roughly where the Nordkinn Peninsula is situated today (Figure 8). Similarly, the Barents Sea Group of northern Varanger, with its complex submarine fan and younger delta, would have been deposited even farther to the northwest. Rocks of the Vardø district, for example, with Timanian structures, are likely to have been located just north of Magerøya, and the Kongsfjord area at least 100 km farther to the northwest on today's continental shelf (Figure 8). The Timanides are considered to have extended even farther to the northwest, to an inferred Balto–Timanian triple junction (Siedlecka et al. 2004, Figure 15), in the vicinity of which the Ediacaran magmatic complexes of the Seiland Igneous Province are thought to have originated (see also Burke et al. 2007). One particular terrane in southernmost Spitsbergen, with Mesoproterozoic protolith ages and carrying evidence of Ediacaran metamorphism, has also been suggested to represent an isolated outlier of the Timanide orogenic belt (Mazur et al. 2009). As the Seiland plutonic rocks now occur in the highest and outermost, Seiland–Sørøy Nappe of the Kalak allochthon, penetrating psammites of Tonian age (Kirkland et al. 2007), then it is not inconceivable that Timanian structures may be found in these thrust sheets, in addition to evidence of possible deformation and metamorphism relating to the *c.* 710 Ma 'Snøfjord event' of Kirkland et al. (2006).

The most westerly segment of the basinal *and* platformal successions on Varanger Peninsula is exposed in one particular area in the Gaissa Nappe southwest of the TKFZ. There, the contact between the Båtsfjord Formation of the Barents Sea Group and the uppermost, Ekkerøya Formation of the Vadsø Group was first considered to be primary (Siedlecka and Siedlecki 1971) but later reinterpreted as tectonic (Johnson et al. 1978, Siedlecki 1980). Subsequently, in 1991, an examination of this contact by a group of geologists from the Geological Survey of Norway and the Russian Academy of Sciences supported the primary contact interpretation. Shortly afterwards, Rice (1994) produced a convincing field documentation of the boundary as being an unconformity. As it is the lower part (Annijokka Member) of the Båtsfjord Formation that is unconformably overlain by the Ekkerøya Formation, this indicates that a large part of the upper Barents Sea Group has either not been deposited in the northwesternmost areas of the Timanian basin

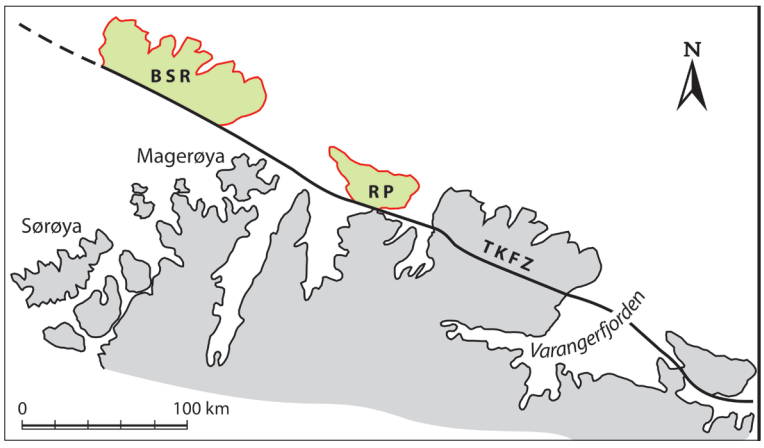

Figure 8. Outline map showing the approximate inferred locations of the Rybachi Peninsula (RP) and the Barents Sea Region (BSR) of Varanger Peninsula prior to their dextral translation along the Trollfjorden–Komagelva and Sredni–Rybachi fault zones in Caledonian (earliest Ordovician) time. Detritus feeding the Båtsnæringen delta from the southwest would have derived from a now concealed, Late Palaeoproterozoic to Mesoproterozoic terrane or a previously transported (Tonian) thrust sheet located some few tens of kilometres to the west or northwest of where Sørøya is situated today.

or has been removed by uplift, tilting and erosion prior to deposition of the prograding, platformal Ekkerøya strata.

The geochemistry of the basinal successions on Rybachi and northern Varanger shows significant differences as compared with the platformal domain. Higher contents of, e.g., Na, Mg, Fe and Ca and a relative deficiency of K point to source terranes dominated by mafic Na-rich complexes of likely volcanic origin (Sochava and Siedlecka 1997). Detrital zircon data from the deltaic Båtsnæringen Formation show a predominance of Mesoproterozoic and Late Palaeoproterozoic detritus and only a minor Neoarchaean component. The same is the case for the subjacent Kongsfjord Formation (Orlov et al. 2011). Accepting that the Båtsnæringen delta was originally situated well to the northwest of Magerøya, the geochemical and zircon data clearly suggest that a Mesoproterozoic, mainly volcanic terrane was exposed to erosion and provided much of the infill of this particular delta. This Mesoproterozoic terrane is not exposed in Finnmark today, and thus likely to be concealed beneath the Caledonian nappes and younger Late Palaeozoic and Mesozoic successions on the continental shelf of the southwestern Barents Sea (Roberts 2007). Alternatively, some of the Mesoproterozoic detritus may have derived from the inferred Tonian-emplaced thrust sheets (Kirkland et al. 2006). Work is in progress on detrital zircon analyses from other formations in both the basinal and the platformal domains, and it is quite conceivable that more evidence of a substantial Mesoproterozoic input may come to light.

Geochemical data from the unconformably overlying Løkviksfjellet Group show a markedly different signature to that in the subjacent Barents Sea Group with high SiO_2 and K_2O contents in mainly quartz-arenitic lithologies (Sochava and Siedlecka 1997), signifying a return to a felsic-magmatic source terrane on the shield to the south or southwest. Detrital zircon data from the Sandfjorden Formation show Late Palaeoproterozoic and Neoarchaean peaks, but also with a minor Mesoproterozoic component.

In summary, taking the full complement of parameters necessary for a comprehensive assessment of the provenances of the latest Mesoproterozoic to Neoproterozoic successions on these four peninsulas, the principal source regions for the fluvial to shallow- and deeper-marine deposits clearly lay at diverse locations to the south (i.e., southwest to southeast). Before post-Caledonian and later denudation events, the platformal sedimentary successions probably extended much farther 'inland' across the Fennoscandian Shield and were most likely fed by several major river systems that dispersed debris northwards from both Neoarchaean and Palaeoproterozoic terranes, and in some cases from Mesoproterozoic sources. Farther to the west or northwest, terranes comprising Mesoproterozoic complexes were also evidently involved in providing debris to the allochthonous, submarine-fan and deltaic formations in northern Varanger Peninsula, as well as to successions in early (Tonian) thrust sheets in the Kalak Nappe Complex farther west (Kirkland et al. 2007). These Mesoproterozoic terranes are inferred to be an integral part of the Precambrian basement concealed beneath the Caledonian Nappes and continental shelf (Roberts 2007, Lorenz et al. 2012). Interestingly, detrital zircons of Mesoproterozoic age sourced on the Fennoscandian Shield are also registered in certain Neoproterozoic sandstone formations in the Timanides of Northwest Russia (Kuznetsov et al. 2010). Some of these zircons were probably recycled from successions in a vast graben and river system that once extended across much of the central Fennoscandian Shield (Kuznetsov et al. 2012).

The thick, submarine fan systems of Rybachi and northern Varanger form the northwestern onshore termination of the 1800 km-long Timanian passive margin, but it has long been speculated as to how much farther northwest the Timan basin actually extended (Siedlecka 1975 and references therein). On Varanger Peninsula, Timanian structures are restricted to the northeasternmost area northeast of the TKFZ (Roberts 1996, Herrevold et al. 2009), but can be traced offshore in aeromagnetic data (Gernigon et al. 2008, Brönner et al. 2009, Gernigon and Brönner 2012) and seabed bathymetric features (Roberts et al. 2011). However, both onland and offshore the Timanian structural grain is quickly overprinted towards the northwest by Caledonian thrusts and folds. Simple restoration of the Barents Sea Group places these Timanian basinal rocks well to the northwest of Magerøya (Figure 8) but since the Neoproterozoic sedimentary wedge attains a thickness of almost 15 km just north of Rybachi Peninsula it is more than likely that the Timanian basin can be found at depth beneath the western Barents Sea.

Conclusions

Assessment of the provenances of Proterozoic successions occurring on four peninsulas flanking the Barents Sea in NE Norway and NW Russia has been carried out based on an evaluation of five disparate parameters. The results indicate the following:-

1. Palaeocurrent data in the pericratonic, platformal areas (Sredni and the Varanger TVR) indicate a principal sediment dispersal from fluvial systems directed between roughly north and northeast, from sources in the Archaean and Palaeoproterozoic terranes of the Fennoscandian Shield. Unconformities beneath specific depositional sequences signify epeirogenic events in the source regions and commonly mark transient changes in current flow. Local input of detritus from a northeasterly source in Mid Vendian time is considered to reflect erosion from the rising deformation front of the Timanide orogen and conversion of the pericratonic shelf into a small foreland basin which is likely to have existed into Early Cambrian time. This synorogenic, foreland basinal feature has also been recognised in the White Sea–Mezen Basin area of

Northwest Russia, immediately southwest of the Timans.
Data from the allochthonous basinal realm of Rybachi and Varanger BSR are also indicative of a general transport towards the northeast, mainly in submarine fans and shelf-edge deltas. These thick successions, representing an extension of the Timanides, were originally located farther to the northwest of where they occur today, with the sources of their detritus now lying concealed beneath the Caledonian nappes and the present-day continental shelf. The Løkviksfjellet Group, which was originally suggested to be of possible Vendian age, was also sourced in the southwest and is likely to be of Cryogenian age. Palaeocurrent data from the Nordkinn Peninsula, part of the Kalak Nappe Complex, also show fairly consistent flow vectors towards N–NW in mainly fluvial to shallow-marine sandstones, but with deeper-water turbidites appearing in the far north.

2. Lithological indicators, including interpretation of depositional systems and their distribution, largely accord with the sediment dispersal patterns on the Rybachi, Sredni and Varanger peninsulas, signifying various sources to the south on the shield. On Rybachi, a spectacular olistostrome-breccia at the base of the succession represents a disintegration and collapse of the fault-bounded shelf-edge footwall.
3. Accumulations of heavy minerals representing palaeoplacer deposits are particularly common on the Sredni and Rybachi peninsulas. A pilot study of such mineral assemblages on Varanger Peninsula showed that at least three provenance areas on the shield, with markedly different abundances of zircon, tourmaline and garnet, have contributed to the Neoproterozoic sedimentary successions. Clear differences are also seen in the heavy-mineral contents of formations on either side of the Trollfjorden–Komagelva Fault Zone. On Nordkinn, concentrations of diverse heavy minerals and notably Ti- and Fe-rich opaques are common as thin beds, foreset strata or lensoid deposits, with probable sources in basement terranes on the shield.
4. A geochemical study of more than 460 samples from the Rybachi, Sredni and Varanger peninsulas has revealed a clear compositional distinction between the basinal and platformal domains, the former with element compositions indicative of likely derivation from mafic to intermediate sources in, e.g., northwestward extensions of the Palaeoproterozoic greenstone complexes, or in terranes farther west in the basement beneath the Caledonian nappes. The transgressive, felsic and silica-rich Løkviksfjellet Group, on the other hand, derives from a markedly different, potassic-granitoid, source region.
5. Detrital mineral isotopic studies (illite and zircon) are few, but those so far available for zircon from Varanger Peninsula denote population peaks in the Mesoproterozoic, Late Palaeoproterozoic and Neoarchaean for sandstones from the platform and from the Tanahorn Nappe, both of which derive from southerly sources. The deltaic Båtsnæringen and submarine-fan Kongsfjord formations in the BSR, however, are quite different in showing a multimodal spread of zircon grains from *c.* 2.1 to 1.0 Ga with only a minor Neoarchaean component. This dominance of Mesoproterozoic detritus, seen in relation to the original location of the delta somewhere to the northwest of Magerøya, argues for the presence of source rocks of this age beneath the Caledonian nappes and continental shelf. These sources could be representative of magmatic or metamorphic complexes which may once have formed part of a northward extension of the Sveconorwegian/Grenvillian orogen, as has been suggested in recent literature, or alternatively represent Tonian-transported sedimentary rocks derived from the margin of Rodinia prior to its ultimate break-up.

Acknowledgements
The authors are grateful to Johan Petter Nystuen and Chris Kirkland for their helpful and constructive comments, as reviewers, and also to Kevin Pickering for his equally helpful suggestions and comments on the manuscript. All these comments helped greatly in allowing us to expand and improve the manuscript. We also thank professors Nikolay Kuznetsov and Elizabeth Miller for providing files of translated publications of papers originally published in Russian, which are valuable additions to our knowledge of the Timanide orogen. We are grateful to Professor Malgorzata Moczydlowska for her written comments on aspects of biostratigraphy. Irene Lundquist is thanked for producing most of the figures, and a special thanks goes to the editor, Trond Slagstad, for allowing us to include Figure 7.

References

Banks, N.L. (1971) *Sedimentological studies in the Late Precambrian and Lower Cambrian rocks of East Finnmark. Unpublished Ph.D. thesis*, University of Oxford, Two volumes.

Banks, N.L. & Røe, S-L. (1974) Sedimentology of the Late Precambrian Golneselva Formation, Varangerfjorden, Finnmark. *Norges geologiske undersøkelse*, **303**, 17–38.

Banks, N.L., Edwards, M.B., Geddes, W.P., Hobday, D.K. and Reading, H.G. (1971) Late Precambrian and Cambro–Ordovician sedimentation in East Finnmark. *Norges geologiske undersøkelse*, **269**, 197–236.

Banks, N.L., Hobday, D.K., Reading, H.G. and Taylor, P.N. (1974) Stratigraphy of the Late Precambrian 'Older Sandstone Series' of the Varangerfjord area, Finnmark. *Norges geologiske undersøkelse*, **303**, 1–15.

Beckholmen, M. and Glodny, J. (2004) Timanian blueschist-facies metamorphism in the Kvarkush metamorphic basement, Northern Urals, Russia. *In* Gee, D.G. and Pease, V. (eds.) *The Neoproterozoic Timanide Orogen of Eastern Baltica*. Geological Society, London, Memoirs, **30**, 125–134.

Be'eri-Shlevin, Y., Gee, D.G., Claesson, S., Ladenberger, A., Kajka, J., Kirkland, C.L., Robinson, P. and Frei, D. (2011) Provenance of Neoproterozoic sediments in the Särv nappes (Middle Allochthon) of the Scandinavian Caledonides: LA–ICP–MS and SIMS U–Pb dating of detrital zircons. *Precambrian Research*, **187**, 181–200.

Burke, K., Roberts, D. and Ashwal, L.D. (2007) Alkaline rocks and carbonatites of northwestern Russia and northern Norway: linked Wilson cycle records extending over two billion years. *Tectonics*, **26**,

Bylund, G. (1994a) Palaeomagnetism of the Late Precambrian Vadsø and Barents Sea Groups, Varanger Peninsula, Norway. *Precambrian Research*, **69**, 81–93.

Bylund, G. (1994b) Palaeomagnetism of Vendian–Early Cambrian sedimentary rocks from E. Finnmark, Norway. *Tectonophysics*, **231**, 45–57.

Cawood, P.A. and Nemchin, A.A. (2001) Paleogeographic development of the east Laurentian margin: constraints from U–Pb dating of detrital zircons in the Newfoundland Appalachians. *Bulletin of the Geological Society of Americ*a, **113**, 1234–1246.

Chapman, T.J. (1980) *The geological evolution of the Laksefjord Nappe Complex, Finnmark, North Norway*. Unpublished Ph.D. thesis, University of Wales, 164 pp.

Daly, J.S., Balagansky, V.V., Timmerman, M.J., Whitehouse, M.J., de Jong, K., Guise, P., Bogdanova, S., Gorbatschev, R. and Bridgwater, D. (2001) Ion microprobe U–Pb zircon geochronology and isotopic evidence supporting a trans-crustal suture in the Lapland–Kola Orogen, northern Fennoscandian Shield. *Precambrian Research*, **105**, 289–314.

Daly, J.S., Balagansky, V.V., Timmerman, M.J. and Whitehouse, M.J. (2006) The Lapland–Kola orogen: Palaeoproterozoic collision and accretion of the northern Fennoscandian lithosphere. *Geological Society, London, Memoirs*, **32**, 579–598.

Drinkwater, N.J., Pickering, K.T. and Siedlecka, A. (1996) Deep-water, fault-controlled sedimentation, Arctic Norway and Russi: response to Late Proterozoic rifting and the opening of the Iapetus Ocean. *Journal of the Geological Society, London*, **153**, 427–436.

Edwards, M.B. (1984) Sedimentology of the Upper Proterozoic glacial record, Vestertana Group, Finnmark, North Norway. *Norges geologiske undersøkelse Bulletin*, **394**, 76 pp.

Edwards, M.B., Baylis, P., Gibling, M., Goffe, W., Potter, M. and Suthren, R.J. (1973) Stratigraphy of the 'Older Sandstone Series' (Tanafjord Group) and Vestertana Group north of Stallogaissa, Laksefjord district, Finnmark. *Norges geologiske undersøkelse*, **294**, 25–41.

Føyn, S. and Siedlecki, S. (1980) Glacial stadials and interstadials of the Late Precambrian Smalfjord Tillite on Laksefjordvidda, Finnmark, North Norway. *Norges geologiske undersøkelse*, **358**, 31–45.

Gaál, G. and Gorbatschev, R. (1987) An outline of the Precambrian evolution of the Baltic Shield. *Precambrian Research*, **35**, 15–52.

Gayer, R.A., Rice, A.H.N., Roberts, D., Townsend, C. and Welbon, A. (1987) Restoration of the Caledonian Baltoscandian margin from balanced cross-sections: the problem of excess continental crust. *Transactions of the Royal Society of Edinburgh, Earth Sciences*, **78**, 197–217.

Gee, D.G. and Pease, V. (editors) (2004) The Neoproterozoic Timanide Orogen of eastern Baltica. *Geological Society of London, Memoirs*, **30**, 255 pp.

Gee, D.G., Fossen, H., Henriksen, N. and Higgins, A.K. (2008) From the Early Palaeozoic platforms of Baltica and Laurentia to the Caledonide Orogen of Scandinavia and Greenland. *Episodes*, **31**, 44–51.

Gorokhov, I.M., Siedlecka, A., Roberts, D., Mel'nikov, N.N. and Turchenko, T.L. (2001) Rb–Sr dating of diagenetic illite in Neoproterozoic shales, Varanger Peninsula, northern Norway. *Geological Magazine*, **138**, 541–562.

Gorokhov, I.M., Mel'nikov, N.N., Negrutsa, V.Z., Turchenko, T.L. and Kutyavin, E.P. (2002) The multistage illite evolution in Upper proterozoic claystones from the Srednii Peninsula, Murmansk coast of the Barents Sea. *Lithology and Mineral Resources*, 37, 162–179.

Grazhdankin, D. (2004) Late Neoproterozoic sedimentation in the Timan foreland. *In* Gee, D.G. and Pease, V. (eds.) *The Neoproterozoic Timanide orogen of Eastern Baltica*. Geological Society, London, Memoirs, **30**, 37–46.

Halverson, G.P., Hoffman, P.F., Schrag, D.P., Maloof, A.C. and Rice, A.H.N. (2005) Toward a Neoproterozoic composite carbon-isotope record. *Bulletin of the Geological Society of America*, **117**, 1181–1207.

Herrevold, T., Gabrielsen, R.H. and Roberts, D. (2009) Structural geology of the southeastern part of the Trollfjorden–Komagelva Fault Zone, Varanger Peninsula, Finnmark, North Norway. *Norwegian Journal of Geology*, **89**, 305–325.

Hobday, D.K. (1974) Interaction between fluvial and marine processes in the lower part of the Late Precambrian Vadsø Group, Finnmark. *Norges geologiske undersøkelse*, **303**, 39–56.

Kirkland, C.L., Daly, J.S. and Whitehouse, M.J. (2006) Granitic magmatism of Grenvillian and Late Neoproterozoic age in Finnmark, Arctic Norway – constraining pre-Scandian deformation in the Kalak Nappe Complex. *Precambrian Research*, **145**, 24–52.

Kirkland, C.L., Daly, J.S. and Whitehouse, M.J. (2007) Provenance and terrane evolution of the Kalak Nappe Complex, Norwegian Caledonides: implications for Neoproterozoic palaeogeography and tectonics. *Journal of Geology*, **115**, 21–41.

Kirkland, C.L., Daly, J.S., Chew, D.M. and Page, L.M. (2008) The Finnmarkian Orogeny revisited: an isotopic investigation in eastern Finnmark, Arctic Norway. *Tectonophysics*, **460**, 158–177.

Kirkland, C.L., Bingen, B., Whitehouse, M.J., Beyer, E. and Griffin, W.L. (2011) Neoproterozoic palaeogeography in the North Atlantic Region: inferences from the Akkajaure and Seve nappes of the Scandinavian Caledonides. *Precambrian Research*, **186**, 127–146.

Koistinen, T., Stephens, M.B., Bogatchev, V., Nordgulen, Ø., Wenner-

ström, M. and Korhonen, J.V. (2001) Geological map of the Fennoscandian Shield, scale 1:2,000,000. *Geological Surveys of Finland, Norway and Sweden, Ministry of Natural Resources of Russia.*

Korja, A., Lahtinen, R. and Nironen, M. (2006) The Svecofennian orogen: a collage of microcontinents and island arcs. *In* Gee, D.G. and Stephenson, R.A. (eds.) *European lithosphere dynamics*. Geological Society of London, Memoirs, **32**, 561–578.

Košler, J., Fonneland, H., Sylvester, P., Tubrett, M. and Pedersen, R-B. (2002) U–Pb dating of detrital zircons for sediment provenance studies – a comparison of laser ablation ICPMS and SIMS techniques. *Chemical Geology*, **182**, 605–618.

Kuznetsov, N.B., Natapov, L.M., Belousova, E.A., Griffin, W.L., O'Reilly, S.Y., Kilikova, K.V., Soboleva, A.A. and Udorotina, O.V. (2010) The first results of U/Pb dating and isotope geochemical studies of detrital zircons from the Neoproterozoic sandstones of the Southern Timan (Djejim–Parma Hill). *Doklady Earth Sciences*, **435** (2), 1676–1683.

Kuznetsov, N.B., Romanyuk, T.V., Shatsillo, A.V., Orlov, S.Y., Golovanova, I.V., Danukalov, K.N. and Ipat'eva, I.S. (2012) The first results of mass U–Pb isotopic dating (LA–ICP–MS) for detrital zircons from the Asha Group, South Urals: paleogeography and paleotectonics. *Doklady Earth Sciences*, **447**, 1240–1246.

Lahtinen, R., Garde, A.A. and Melezhik, V.A. (2008) Paleoproterozoic evolution of Fennoscandia and Greenland. *Episodes*, **31**, 20–28.

Laird, M.G. (1972) Sedimentation of the Late Precambrian Raggo Group, Varanger Peninsula, Finnmark. *Norges geologiske undersøkelse*, **278**, 1–11.

Larionov, A.N., Andreichev, V.A. and Gee, D.G. (2004) The Vendian alkaline igneous suite of northern Timan: ion microprobe U–Pb zircon ages of gabbros and syenite. *In* Gee, D.G. and Pease, V. (eds.) *The Neoproterozoic Timanide Orogen of Eastern Baltica*. Geological society, London, Memoirs, **30**, 69–74.

Levell, B.K. (1978) *Sedimentological studies in the Late Precambrian Løkvikfjell Group, North Norway.* Unpublished D.Phil. thesis, University of Oxford, 328 pp.

Levchenkov, O.A., Levsky, L.K., Nordgulen, Ø., Dobrzhinetskaya, L.F., Vetrin, V.R., Cobbing, J., Nilsson, L.P. and Sturt, B.A. (1995) U–Pb zircon ages from Sørvaranger, Norway, and the western part of the Kola Peninsula, Russia. *Norges geologiske undersøkelse Special Publication*, **7**, 29–47.

Lorenz, H., Gee, D.G., Larionov, A.N. and Majka, J. (2012) The Grenville–Sveconorwegian orogen in the high Arctic. *Geological Magazine*,

Lyubtsov. V.V., Mikhailova, N.S. and Predovsky, A.A. (1989) *Lithostratigraphy and microfossils of the Late Precambrian in the Kola Peninsula*. Apatity, 129 pp. (in Russian).

Lyubtsov, V. V., Predovsky, A. A., Negrutsa, V. Z., Siedlecka, A. and Roberts, D. (1999) Neoproterozoic sedimentary rock successions of the Barents and White Sea coasts of the Kola Peninsula, Northwest Russia. *Norges geologiske undersøkelse Report 99–138*, 91 pp.

Mazur, S., Czerny, J., Majka, J., Manecki, M, Holm, D., Smyrak, A. and Wypych, A. (2009) A strike-slip terrane boundary in Wedel Jarlsberg Land, Svalbard, and its bearing on correlations of SW Spitsbergen with the Pearya terrane and Timanide belt. *Journal of the Geological Society, London*, **166**, 529–544.

Morton, A.C. and Hallsworth, C.R. (1994) Identifying provenance-specific features of detrital heavy mineral assemblages in sandstones. *Sedimentary Geology*, **90**, 241–256.

Morton, A.C. and Hallsworth, C.R. (1999) Processes controlling the composition of heavy mineral assemblages in sandstones. *Sedimentary Geology*, **124**, 3–29.

Morton, A.C., Claoué-Long, J.C. and Berge, C. (1996) SHRIMP constraints on sediment provenance and transport history in the Mesozoic Statfjord Formation, North Sea. *Journal of the Geological Society, London*, **153**, 915–929.

Morton, A.C., Hallsworth, C. and Chalton, B. (2004) Garnet compositions in Scottish and Norwegian basement terrains: a framework for interpretation of North Sea sandstone provenance. *Marine and Petroleum Geology*, **21**, 393–410.

Morton, A.C., Whitham, A.G. and Fanning, C.M. (2005) Provenance of Late Cretaceous to Paleocene submarine fan sandstones in the Norwegian Sea: integration of heavy mineral, mineral chemical and zircon age data. *Sedimentary Geology*, **182**, 3–28.

Negrutsa, V.Z. (1971) Stratigraphy of the Hyperborean deposits of the Sredni and Rybachi Peninsulas and the Kildin Island. In Problems of Precambrian geology of the Baltic Shield and the Russian platform cover. *VSEIGEI*, **175**, 153–186. (in Russian)

Negrutsa, V.Z., Basalaev, A.A. and Chikirev, I.V. (1995) Phosphorites of the Upper Proterozoic sediments of the Sredni, Rybachi and Varanger Peninsulas. *Norges geologiske undersøkelse Special Publication*, **7**, 297–305.

Nicoll, G.R., Tait, J.A. and Zimmerman, U. (2009) Provenance analysis and tectonic setting of Neoproterozoic sediments on the Varanger Peninsula, northern Norway. (abstract) *Fermor Meeting, Edinburgh, Scotland, Abstract Volume*, p. 68.

Olovyanishnikov, V.G., Roberts, D. and Siedlecka, A. (2000) Tectonics and sedimentation of the Meso- to Neoproterozoic Timan–Varanger Belt along the northeastern margin of Baltica. *Polarforschung*, **68**, 267–274.

Orlov, S.Y., Kuznetsov, N.B., Miller, E.L., Soboleva, A.A. and Udoratina, O.V. (2011) Age constraints for the pre-Uralide–Timanide orogenic event inferred from the study of detrital zircons. *Doklady Earth Sciences*, **440**, 1216–1221.

Pease, V. and Scott, R.A. (2009) Crustal affinities in the Arctic Uralides, northern Russia: significance of detrital zircon ages from Neoproterozoic and Palaeozoic sediments in Novaya Zemlya and Taimyr. *Journal of the Geological Society, London*, **166**, 517–527.

Pickering, K.T. (1981) The Kongsfjord Formation – a Late Precambrian submarine fan in north-east Finnmark, North Norway. *Norges geologiske undersøkelse*, **367**, 77–104.

Pickering, K.T. (1982a) A Precambrian upper basin-slope and prodelta

in northeast Finnmark, North Norway – a possible ancient upper continental slope. *Journal of Sedimentary Petrology*, **52**, 171–186.

Pickering, K.T. (1982b) Middle-fan deposits from the late Precambrian Kongsfjord Formation Submarine Fan, northeast Finnmark, northern Norway. *Sedimentary Geology*, **33**, 79–110.

Pickering, K.T. (1983) Transitional submarine-fan deposits from the late Precambrian Kongsfjord Formation submarine fan, NE. Finnmark, N. Norway. *Sedimentology*, **30**, 181–199.

Pickering, K.T. (1985) Kongsfjord turbidite system, Norway. *In:* Bouma, A.H., Normark, W.R. and Barnes, N.E. (eds.) *Submarine fans and related turbidite systems*. Springer, New York, 237–244.

Reading, H.G. (1965) Eocambrian and Lower Palaeozoic geology of the Digermul Peninsula, Tanafjord, Finnmark. *Norges geologiske undersøkelse*, **234**, 167–191.

Reading, H.G. and Walker, R.G. (1966) Sedimentation of Eocambrian tillites and associated sediments in Finnmark, northern Norway. *Palaeogeography, Palaeoclimatology, Palaeoecology*, **2**, 177–212.

Rice, A.H.N. (1994) Stratigraphic overlap of the Late Precambrian Vadsø and Barents Sea Groups and correlation across the Trollfjorden–Komagelva Fault, Finnmark, North Norway. *Norsk Geologisk Tidsskrift*, **74**, 48–57.

Rice, A.H.N. and Roberts, D. (1988) Multi-textured garnets from a single growth event: and example from northern Norway. *Journal of Metamorphic Geology*, **6**, 159–172.

Rice, A.H.N. and Roberts, D. (1995) Very low-grade metamorphism of Upper Proterozoic sedimentary rocks of the Rybachi and Sredni Peninsulas and Kildin Island, NE Kola region, Russia. *Norges geologiske undersøkelse Special Publication*, **7**, 259–269.

Rice, A.H.N. and Frank, W. (2003) The early Caledonian (Finnmarkian) event reassessed in Finnmark: $^{40}Ar/^{39}Ar$ cleavage age data from NW Varangerhalvøya, N. Norway. *Tectonophysics*, **374**, 219–236.

Rice, A.H.N., Gayer, R.A., Robinson, D. & Bevins, R.E. (1989) Strike-slip restoration of the Barents Sea Caledonides terrane, Finnmark, North Norway. *Tectonics*, **8**, 247–264.

Rice, A.H.N., Hofmann, C.-C. and Pettersen, A. (2001) A new sedimentary succession from the southern margin of the Gaissa Basin, South Varangerfjord, North Norway. *Norwegian Journal of Geology*, **81**, 41–48.

Rice, A.H.N., Edwards, M.B., Hansen, T.A., Arnaud, E. and Halverson, G.P. (2011) Glaciogenic rocks of the Neoproterozoic Smalfjord and Mortensnes formations, Vestertana Group, E. Finnmark, Norway. *Geological Society of London, Memoirs,* **36**, 593–602.

Roberts, D. (1972) Tectonic deformation in the Barents Sea region of Varanger Peninsula, Finnmark. *Norges geologiske undersøkelse*, 282, 39 pp.

Roberts, D. (1995) Principal features of the structural geology of Rybachi and Sredni Peninsulas, and some comparisons with Varanger Peninsula. *Norges geologiske undersøkelse Special Publication*, **7**, 247–258.

Roberts, D. (1996) Caledonian and Baikalian tectonic structures on Varanger Peninsula, Finnmark, and coastal areas of Kola Peninsula, NW Russia. *Norges geologiske undersøkelse Bulletin*, **431**, 59–65.

Roberts, D. (2007) Palaeocurrent data from the Kalak Nappe Complex, northern Norway: a key element in models of terrane affiliation. *Norwegian Journal of Geology*, **87**, 319–328.

Roberts, D. and Andersen, T.B. (1985) Nordkapp. Description to the 1:250,000 bedrock-geological map. (in Norwegian with a 5-page summary in English) *Norges geologiske undersøkelse Skrifter*, **61**, 49 pp.

Roberts, D. and Gee, D.G. (1985) An introduction to the structure of the Caledonides. *In* Gee, D.G. and Sturt, B.A. (eds.) *The Caledonide Orogen – Scandinavia and related areas*. John Wiley & Sons, Chichester, 55–68.

Roberts, D. and Siedlecka, A. (2002) Timanian orogenic deformation along the northeastern margin of Baltica, Northwest Russia and Northeast Norway, and Avalonian–Cadomian connections. *Tectonophysics*, **352**, 169–184.

Roberts, D. and Olovyanishnikov, V. (2004) Structural and tectonic development of the Timanide orogen. *In* Gee, D.G. and Pease, V. (eds.) *The Neoproterozoic Timanide Orogen of Eastern Baltica*. Geological Society, London, Memoirs, **30**, 47–57.

Roberts, D., Davidsen, B. and Slagstad, T. (2008) Detrital zircon age record of platformal and basinal Neoproterozoic sandstones from Varanger Peninsula, North Norway: a preliminary study. (abstract and poster) *European Geosciences Union, General Assembly, Vienna April 2008*.

Roberts, D., Chand, S. and Rise, L. (2011) A half-graben of inferred Late Palaeozoic age in outer Varangerfjorden, Finnmark: evidence from seismic-reflection profiles and multibeam bathymetry. *Norwegian Journal of Geology*, **91**, 191–200.

Røe, S.-L. (1970) Correlation between the Late Precambrian Older Sandstone Series of the Tanafjord and Varangerfjord areas: preliminary report. *Norges geologiske undersøkelse*, **266**, 230–245.

Røe, S.-L. (1975) *Stratification, sedimentary processes and depositional environments of part of the Late Precambrian Vadsø group, Varanger fjord area, Finnmark.* Unpublished Cand. Real. thesis, University of Bergen, 187 pp.

Røe, S.-L. (2003) Neoproterozoic peripheral-basin deposits in eastern Finnmark, northern Norway: stratigraphic revision and palaeotectonic implications. *Norwegian Journal of Geology*, **83**, 259–274.

Samuelsson, J. (1997) Biostratigraphy and palaeobiology of Early Neoproterozoic strata of the Kola Peninsula, Northwest Russia. *Norsk Geologisk Tidsskrift*, **77**, 1–28.

Schatsky, N.S. (1952) On the Proterozoic/Palaeozoic boundary and the Riphean deposits on the Russian Platform. *Izvestiia Akademii nauk SSSR, Seriia geologicheskaia*, **5**, 36–49. [in Russian]

Siedlecka, A. (1972) Kongsfjord Formation – a Late Precambrian flysch sequence from the Varanger Peninsula, Finnmark. *Norges geologiske undersøkelse*, **278**, 41–80.

Siedlecka, A. (1978) Late Precambrian tidal-flat deposits and algal stromatolites in the Båtsfjord Formation, East Finnmark, North Norway. *Sedimentary Geology*, **21**, 177–210.

Siedlecka, A. (1985) Development of the Upper Proterozoic sedimentary basins of the Varanger Peninsula, East Finnmark, North Norway. *Bulletin of the Geological Survey of Finland*, **331**, 175–185.

Siedlecka, A. (1995) Major element geochemistry of Upper Proterozoic greywackes from Norway and a coastal area of the Kola Peninsula in northern Russia. *Norges geologiske undersøkelse Special Publication*, **7**, 285–296.

Siedlecka, A. and Siedlecki, S. (1971) Late Precambrian sedimentary rocks of the Tanafjord–Varangerfjord Region of Varanger Peninsula, northern Norway. *Norges geologiske undersøkelse*, **209**, 246–294.

Siedlecka, A. and Edwards, M.B. (1980) Lithostratigraphy and sedimentation of the Riphean Båsnæring Formation, Varanger Peninsula, North Norway. *Norges geologiske undersøkelse*, **355**, 27–47.

Siedlecka, A. and Roberts, D. (1992) The bedrock geology of Varanger Peninsula, Finnmark, North Norway: an excursion guide. *Norges geologiske undersøkelse Special Publication*, **5**, 45 pp.

Siedlecka, A. and Lyubtsov, V.V. (1997) Heavy mineral assemblages in the Neoproterozoic rocks of the Varanger Peninsula, North Norway: a pilot project. (extended abstract). *Norges geologiske undersøkelse Bulletin*, **433**, 26–27.

Siedlecka, A., Pickering, K.T. and Edwards, M.B. (1989) Upper Proterozoic passive margin deltaic complex, Finnmark, N. Norway. *In:* Whateley, M.K.G. and Pickering, K.T. (eds.) *Geological Society of London, Special Publication*, **41**, 205–219.

Siedlecka, A., Lyubtsov, V.V. and Negrutsa, V.Z. (1995a) Correlation between Upper Proterozoic successions in the Tanafjorden–Varangerfjorden Region of Varanger Peninsula, northern Norway, and on Sredni Peninsula and Kildin Island in the northern coastal areas of Kola Peninsula in Russia. *Norges geologiske undersøkelse Special Publication*, **7**, 217–232.

Siedlecka, A., Negrutsa, V.Z. and Pickering, K.T. (1995b) Upper Proterozoic turbidite system of the Rybachi Peninsula, northern Russia – a possible stratigraphic counterpart of the Kongsfjord Submarine Fan of the Varanger Peninsula, northern Norway. *Norges geologiske undersøkelse Special Publication*, **7**, 201–216.

Siedlecka, A., Roberts, D., Nystuen, J.P. and Olovyanishnikov, V.G. (2004) Northeastern and northwestern margins of Baltica in Neoproterozoic time: evidence from the Timanian and Caledonian orogens. *In* Gee, D.G. and Pease, V. (eds.) *The Neoproterozoic Timanide orogen of eastern Baltica*. Geological Society, London, Memoirs **30**, 169–190.

Siedlecki, S. (1980) Geologisk kart over Norge, berggrunnskart, VADSØ – M. 1:250.000. *Norges geologiske undersøkelse*.

Slagstad, T., Roberts, D. and Davidsen, B. (2011) Provenance study of selected Neoproterozoic sandstone formations from Varanger Peninsula, Finnmark: preliminary results. (Abstract) *Norsk Geologisk Førening, Abstracts and Proceedings, Vinterkonferansen 2011*, 90–91.

Sochava, A.V. (1995) Petrochemistry of the Upper Precambrian deposits from the Sredni and Rybachi Peninsulas and comparison with correlative sequences from the Timans and Urals. *Norges geologiske undersøkelse Special Publication*, **7**, 271–283.

Sochava, A.V. and Siedlecka, A. (1997) Major element geochemistry of Neoproterozoic successions of Varanger Peninsula, North Norway, and Sredni and Rybachi Peninsulas, Northwest Kola, Russia: provenance patterns and basin evolution. *Norges geologiske undersøkelse Bulletin*, **432**, 77–93.

Sokolov, B.S. (1952) Age constraints of the oldest sedimentary cover of the Russian Platform. *Izvestiia akademii nauk SSSR, Seriia geologicheskaia*, **5**, 21–31. [in Russian]

Tschernyschev, F.N. (1901) On the geological structure of the Timans and on relation of the Timan Fault to other regions of northern Europe. *Zapiski Russiskogo Mineralogicheskogo Obshchestva*, **34**, 29–33. [in Russian]

Vidal, G. and Siedlecka, A. (1983) Planktonic, acid-resistant microfossils from the Upper Proterozoic strata of the Barents Sea Region of Varanger Peninsula, Finnmark, northern Norway. *Norges geologiske undersøkelse*, **382**, 145–179.

Williams, G.D. (1974) Sedimentary structures in the amphibolite-facies rocks of the Bekkarfjord Formation, Laksefjord, Finnmark. *Norges geologiske undersøkelse*, **311**, 35–48.

RESEARCH ARTICLE

Geology of the Båtsfjordfjellet drillcore, Varanger Peninsula, Finnmark, northern Norway

Anna Siedlecka and David Roberts*

Geological Survey of Norway, P.O.Box 6315 Sluppen, 7491 Trondheim, Norway.
**david.roberts@ngu.no*

Logging of >800 metres of drillcore from a borehole on Båtsfjordfjellet, Varanger Peninsula, revealed a succession of very low-grade, metasedimentary rocks which are assigned to specific Neoproterozoic formations recognisable from regional mapping. The lowest 320 metres of the core consist largely of laminated, maroon to greenish-grey mudstones with thin sandstone beds and some dolomite, characteristic of the Skovika Member of the Båtsfjord Formation. A weak spaced cleavage is present in the mud- and clay-rich lithologies. This pelitic unit is overlain across an inferred unconformity by *c.* 230 m of coarse-grained sandstones with small-clast conglomerates, representing the Sandfjorden Formation of the Løkviksfjellet Group. The upper *c.* 240 m of the drillcore comprise a repetition of the Skovika Member mudrocks, with the basal contact against the Sandfjorden Formation sandstones marked by a thrust fault which appears to have been reactivated by normal fault movements.

Introduction

In mainland Norway, boreholes drilled solely for scientific purposes are a rarity. In recent years, however, two such holes have been drilled in Finnmark as part of a collaborative NGU–Statoil project – termed the 'HeatBar Project' – aimed at quantifying the heat production and flow from diverse basement rocks which are known to occur beneath the Late Palaeozoic to Cenozoic sedimentary basins of the western Barents Sea. The two drillholes are located (a) on Båtsfjordfjellet, a few kilometres southwest of the small town of Båtsfjord, in the northern part of Varanger Peninsula; and (b) at lake Vuoddašjavri, on Finnmarksvidda, *c.* 50 km northeast of Kautokeino (Pascal et al. 2008, 2010).

The Vuoddašjavri hole was drilled vertically in 2008 in Neoarchaean to Palaeoproterozoic gneisses and amphibolites down to a depth of *c.* 767 metres. By contrast, the drillhole on Båtsfjordfjellet (Figure 1), drilled in 2005, penetrated low-grade metasedimentary rocks of the Neoproterozoic, Barents Sea and

Siedlecka, A. and Roberts, D. (2012) Geology of the Båtsfjordfjellet drillcore, Varanger Peninsula, Finnmark, northern Norway. *Norges geologiske undersøkelse Bulletin*, **452**, 20-29.

Løkviksfjellet groups, initially reaching a vertical depth of 800 metres, but later collapsing at c. 620 m depth. The two boreholes and the extracted drillcores were subsequently logged for a variety of parameters, e.g., lithologies, thermal conductivity and diffusivity, rock density, gamma countings, temperature profile, etc., full details of which are contained in a NGU report (Pascal et al. 2010).

The purpose of the present contribution is to record the geology and some of the sedimentological and microstructural features resulting from our lithological logging of approximately 800 m of drillcore from the Båtsfjordfjellet site, and examination of thin-sections of eighteen representative rock samples from the core. As this is the first borehole to have been drilled on Varanger Peninsula and, in fact, in the northern Norwegian Caledonides as a whole, the logged data are clearly exclusive and thus worthy of documentation – moreso as details of our comprehensive logging and petrographic study were, by pure oversight, not included in the above-cited NGU reports.

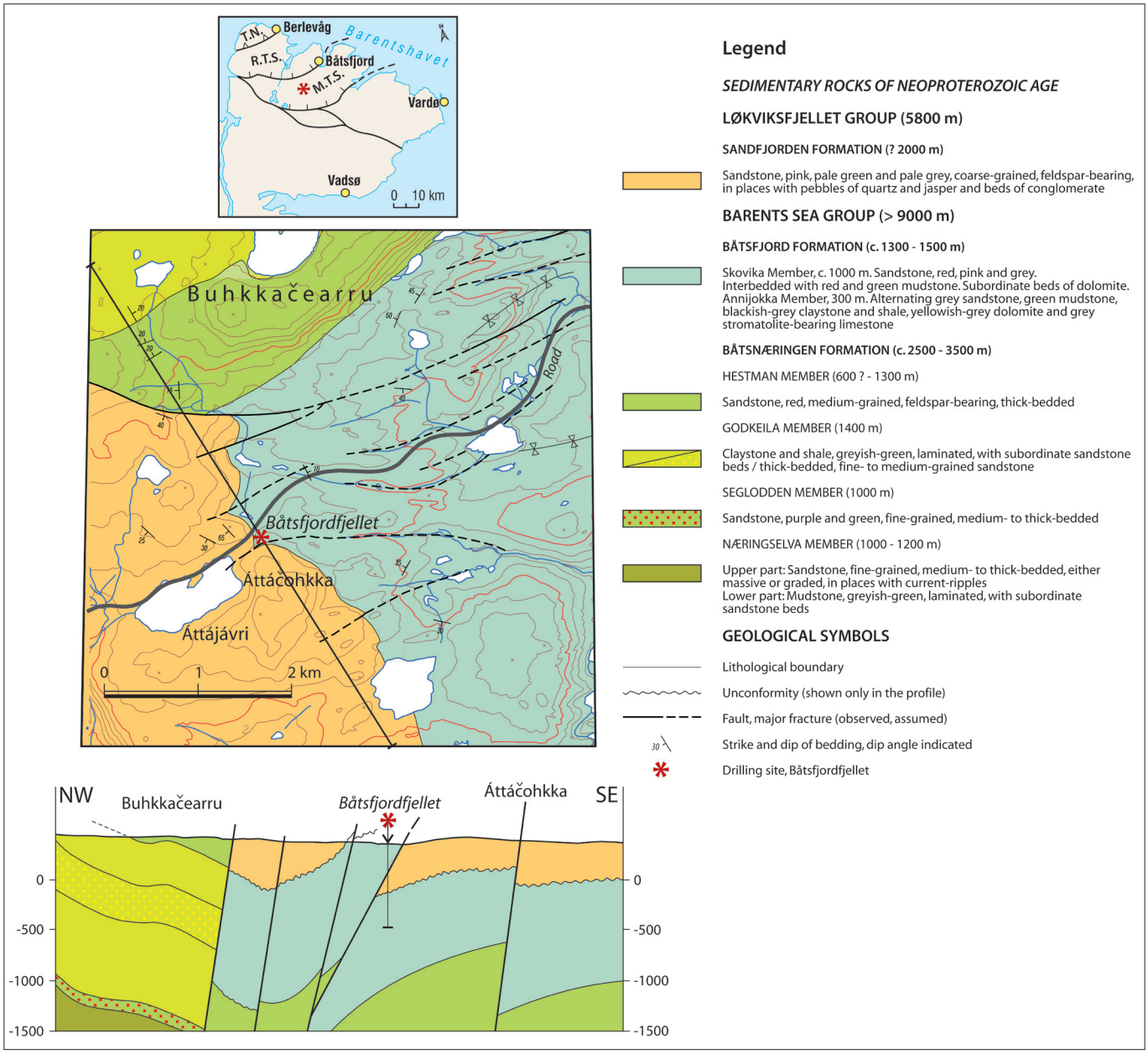

Figure 1. Location of the Båtsfjordfjellet borehole, and simplified map and profile of the local geology, Varanger Peninsula. In the inset map, M.T.S – Máhkirčearru thrust sheet; R.T.S. – Rákkočearru thrust sheet; T.N. – Tanahorn Nappe.

The Båtsfjordfjellet drillcore

Most of the drillcore is of good quality but some parts have been reduced to rubble. In some intervals, parts of the core are missing. In addition, the depths marked on the wooden drillcore boxes are in some cases incorrect, judging from our own measurements of continuous lengths of drillcore. Because of this, the intervals indicated in our description should be regarded only as our best estimates.

Lithologies and lithostratigraphy

The borehole penetrated parts of two, Neoproterozoic, lithostratigraphic units which are known to occur over large areas of northern Varanger Peninsula: the *Skovika Member* of the Båtsfjord Formation (part of the Barents Sea Group) and the *Sandfjorden Formation* (part of the Løkviksfjellet Group). The general lithostratigraphy of the Barents Sea Region of Varanger Peninsula is indicated in Figure 2, modified from Siedlecka and Roberts (1992). The following units have been measured and identified, in descending order, summarised in Figure 3:

Båtsfjord Formation, Skovika Member

c. 240 m with average dip 70°, equivalent to *c.* 100 m of stratigraphic section.

Sandfjorden Formation

c. 240 m with average dip 30°, equivalent to *c.* 210 m of stratigraphic section.

Båtsfjord Formation, Skovika Member

c. 321 m with average dip 25°, equivalent to *c.* 290 m of stratigraphic section.

Sum 801 m, = *c.* 600 m of stratigraphic section.

It has not been possible to indicate precisely which parts of the named lithostratigraphic units have been penetrated by the drillhole.

The intervals of the drillcore where contacts between the recognisable lithostratigraphic units occur are unfortunately either incomplete or partly represented by rubble (see the core log description, Appendix 1). The lower of the two contacts, between the Sandfjorden Formation and the subjacent Skovika Member, is considered to represent an unconformity, based on the fact that there is a well known, regional, low-angle, angular unconformity separating the Barents Sea Group from the Løkviksfjellet Group (Siedlecki and Levell 1978). The upper contact, between the Sandfjorden Formation and the overlying but older Skovika Member, is marked by a clay gouge and is interpreted as an original thrust-fault of unknown geometry and age. However, there are reasons for believing that this thrust-fault is most likely a Caledonian structure (p. 26) which was later reactivated in a more brittle, and probably extensional regime, thus generating the gouge.

The **Skovika Member** is lithologically heterogeneous, consisting of sandstones, mudstones, clay-rich rocks and dolomite metamorphosed at very low grade (Rice et al. 1989) (Figure 4a, b, d). The rocks are fine- to very fine-grained and in several places their textures extend across the classification boundaries of siliciclastic terrigenous rocks based on grain size, e.g., mud, clay or sand. Porosity varies, however, as in many places in the core the sand-rich varieties are comparatively porous. The pelitic rocks are characterised by a variegated coloration – greenish-grey, maroon or dark pink (Figure 4). The maroon and pink varieties contain disseminated hematite, whereas the grey sediments do not and are usually dolomitic.

Some fairly homogeneous sandstone beds are present but, in general, the rocks are finely laminated where sand-, mud- or clay-sized particles or dolomite form a predominant component. Microscopic examination shows that silt and fine- to medium-grained sand are primarily represented by quartz with only subordinate grains of feldspar and sporadic flakes of chlorite (Figure 5). Clay-sized particles are a mixture of muscovite-like phyllosilicates described here as sericite, but some could be illite. This is a clastic material and a weathering product of silicate minerals derived from different source rocks. The dolomite is very fine-grained to micritic and is authigenic, either primary or a diagenetic replacement product of a calcium-carbonate mineral (calcite and/or aragonite).

In many of the finer-grained layers and laminae there is a weak spaced cleavage developed at a very low angle (normally 5–20°) to the primary layering. Where the cleavage folia cut

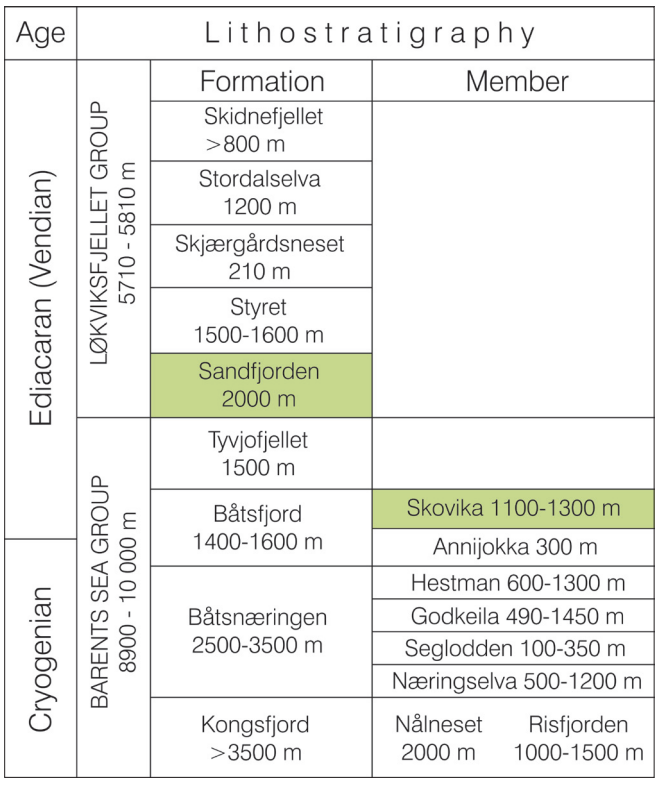

Figure 2. Lithostratigraphy of the Barents Sea and Løkvikfjellet groups, Barents Sea Region of Varanger Peninsula. N.B. – see Addendum, p. 27.

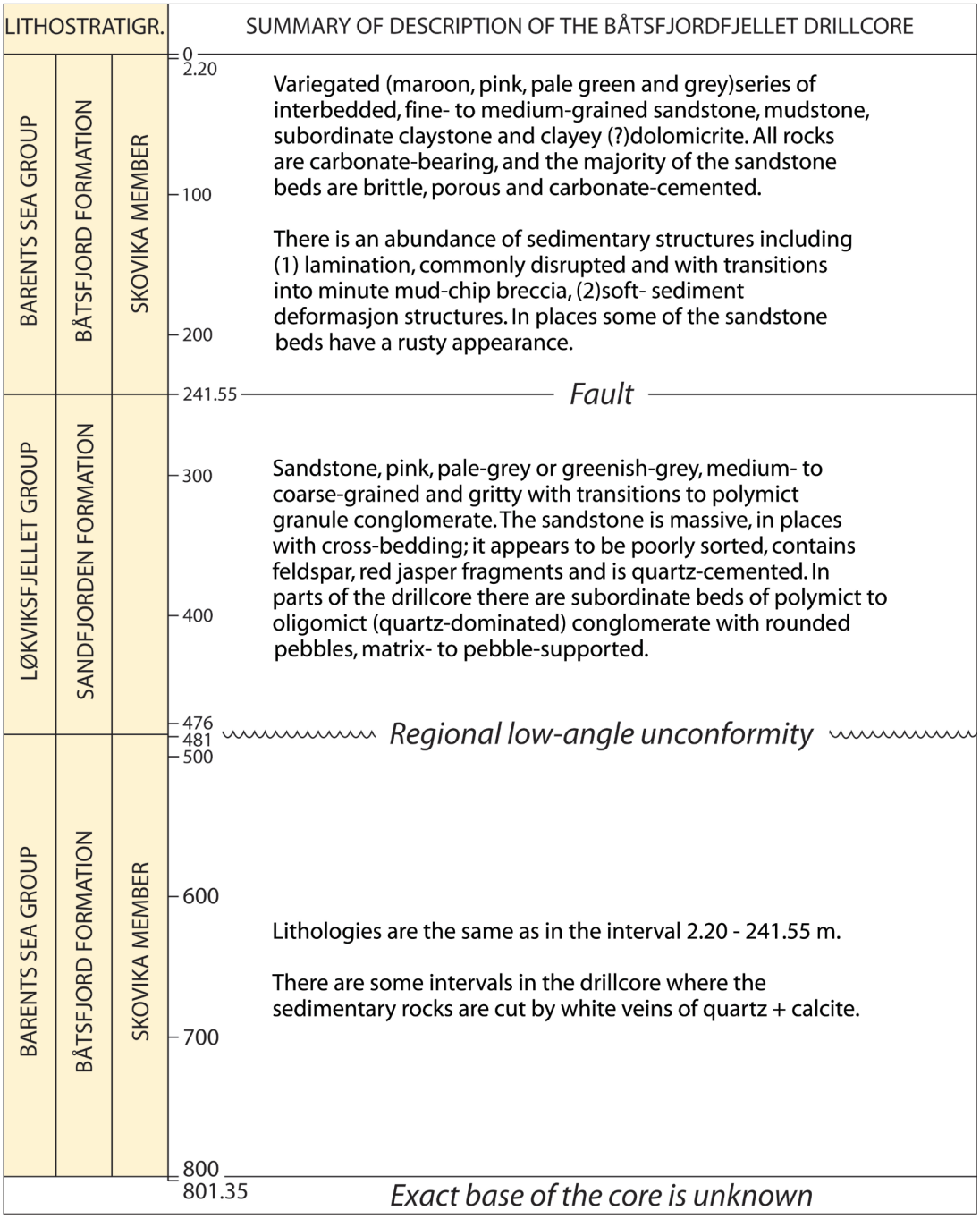

Figure 3. Summary description of the Båtsfjordfjellet drillcore.

obliquely through quartz-rich laminae, the quartz grains show clear evidence of dissolution on the sides in contact with the cleavage surfaces, and tails or beards of microcrystalline material are developed in the pressure-shadow areas around the quartz grains. In other cases, very fine-grained layers or laminae show features indicative of layer-normal compaction. The oblique spaced cleavage is assumed to be axial planar to small folds that can be seen in outcrop in many parts of the Båtsfjord Formation; but no folds have been observed in our thin-sections. A summary description of the thin-sections is given in Appendix 2.

The **Sandfjorden Formation** is lithologically fairly homogeneous, consisting of coarse- to very coarse-grained, well sorted sandstones with subordinate granule- and small-pebble conglomerates (Figure 4c), also metamorphosed at very low grade. In spite of the largely oligomict character of the conglomerates and the apparently feldspathic character of the sandstones (Figure 5), the rocks in fact consist mostly of quartz with some grains or small clasts of quartzite, sandstone, chert, red jasper and sporadic feldspar. Some horizons contain enhanced contents of K-feldspar. The quartz grains are subrounded to well

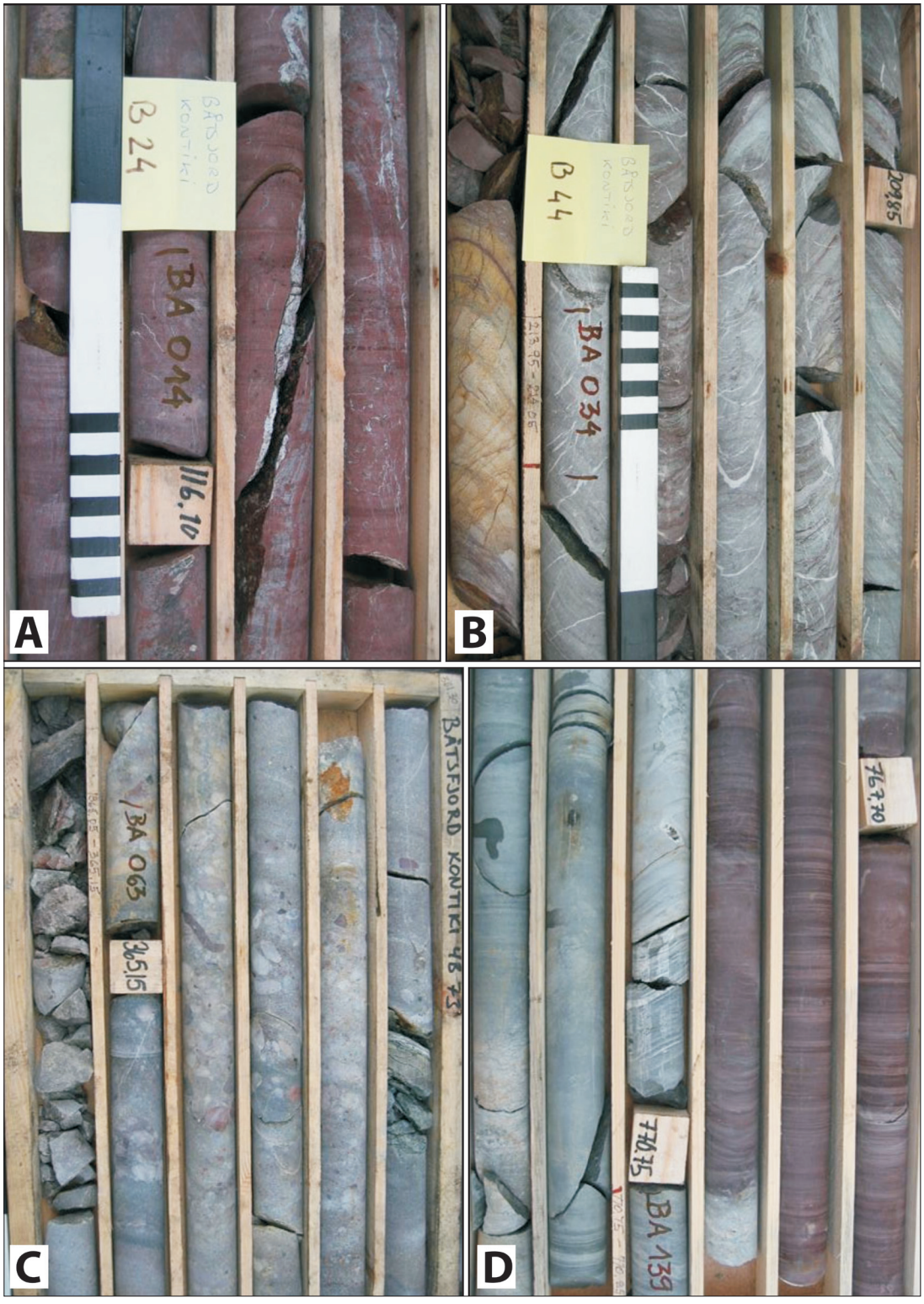

Figure 4. Selected core sections from different boxes. See Appendix 1 for logged descriptions. (a) Laminated maroon mudstones of the Skovika Member; part of box B24. (b) Laminated, grey, silty sandstone and intercalations of mudstone, with yellowish-grey limonitic sandstone to the left; Skovika Member, box B44. (c) Conglomerate, mostly oligomict with quartz pebbles, but also small scattered clasts of jasper; Sandfjorden Formation, box B73. (d) Maroon laminated mudstone in the three core sections to the right. The three cores to the left consist mostly of grey fine-grained sandstone and mudstone; Skovika Member, box B150.

rounded and in places exhibit quartz overgrowths (Figure 5). These overgrowths are probably more common than is possible to observe in small thin-sections (because of the clean grain surfaces) and have evidently contributed to the tightly packed texture of the sandstones. Some of the quartz grains, however, have thin skins of a sericitic cement.

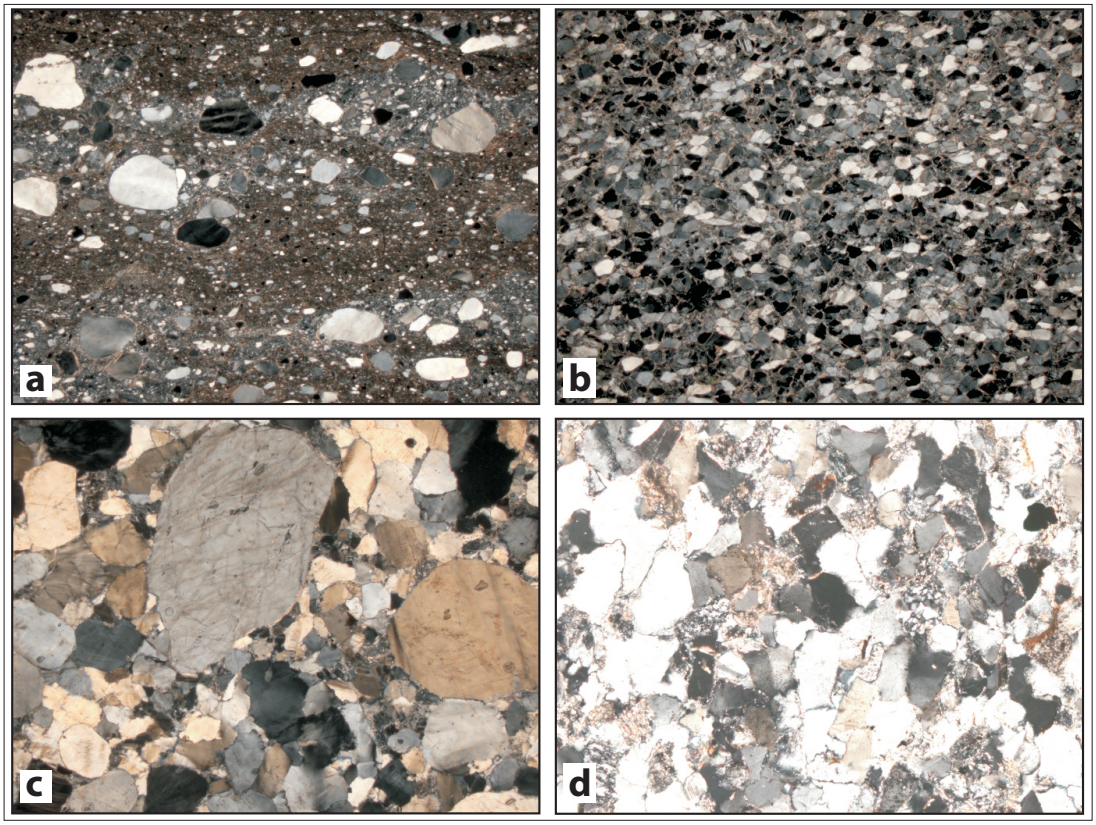

Figure 5. Photomicrographs of selected thin-sections. Brief descriptions of each thin-section are given in Appendix 2. (a) BA 033, mudstone with large subrounded quartz grains of probable eolian origin. Skovika Member. Magn. x10. (b) BA 033, fine-grained sandstone; Skovika Member. Magn. x5. (c) BA 047, coarse-grained, gritty, quartz sandstone, Sandfjorden Formation. Magn. x5. (d) BA 005, fine-grained quartz sandstone with sericitic matrix, Skovika Member. Magn. x10.

Lithology, thermal conductivity and gamma radiation

It is interesting to compare the logged lithologies with profiles of thermal conductivity and gamma radiation recorded in the Båtsfjordfjellet borehole. Rocks of the **Skovika Member** show a thermal conductivity in the range 2–5.5 W m^{-1} K^{-1}, the lowest values being typical for the mud-dominated lithologies (Figure 6b) (Pascal et al. 2010). The subordinate fine-grained sandstones, which also yield fairly low thermal conductivity values, are either mud-enriched or contain mud laminae. The mudstones with the fairly high conductivity values are most probably silt-rich varieties. The presence of dolomite does not seem to have had any effect on the thermal conductivity values. These opinions, however, are based on only eighteen samples examined in thin-section out of a total of 146 samples taken for conductivity measurements. The overlap between the conductivities of rocks coded as 'sandstone' or 'mudstone' reflects the commonly observed transitional character between these two rock types. Sandstones and silt-rich mudstones are rich in quartz, and in addition to the texture and grain size this appears to be the reason why the sandstones and some of the mudstones exhibit values mostly between 3 and 4 W m^{-1} K^{-1}.

With few exceptions, the rocks of the **Sandfjorden Formation** show thermal conductivity values from 5 to slightly above 6 W m^{-1} K^{-1} (Figure 6b) (Pascal et al. 2010). This is a reflection of the quartz-dominated mineralogy combined with grain size, and perhaps also of the low porosity of these rocks. Four samples classified as sandstones show considerably lower conductivities and the same is noted in three mudstone samples close to the base of the formation. The four anomalous sandstone samples are, in fact, associated with mudstones and may perhaps contain slightly more mud than in the remainder of the examined, quartz-dominated, core section of the formation. The presence of mudstones close to the base of the formation may be explained by the regional, erosional character of the contact against the underlying, finer-grained and mud-rich Skovika Member.

A gamma log shows higher radiation values for the pelite-dominated Skovika Member as compared with the quartz-rich Sandfjorden Formation (Figure 6a). This clear distinction is taken to relate to the abundance of K-rich clay minerals in the Skovika mudstones. Whilst low values of gamma characterise the Sandfjorden sandstones, increased values towards the middle of the unit may correlate with an increased content of K-feldspar or proportionally more mudstone intercalations.

In summary, it is apparent that the high thermal conductivity values are characteristic of the coarse, 'clean', quartz sandstones and conglomerates with tightly packed, rounded grains and a restricted, comparatively low porosity. This feature goes hand in hand with low values of gamma radiation. On the contrary, the lower conductivity values seem to be more typical for the finer-grained, polymineralic, mud-enriched rocks where,

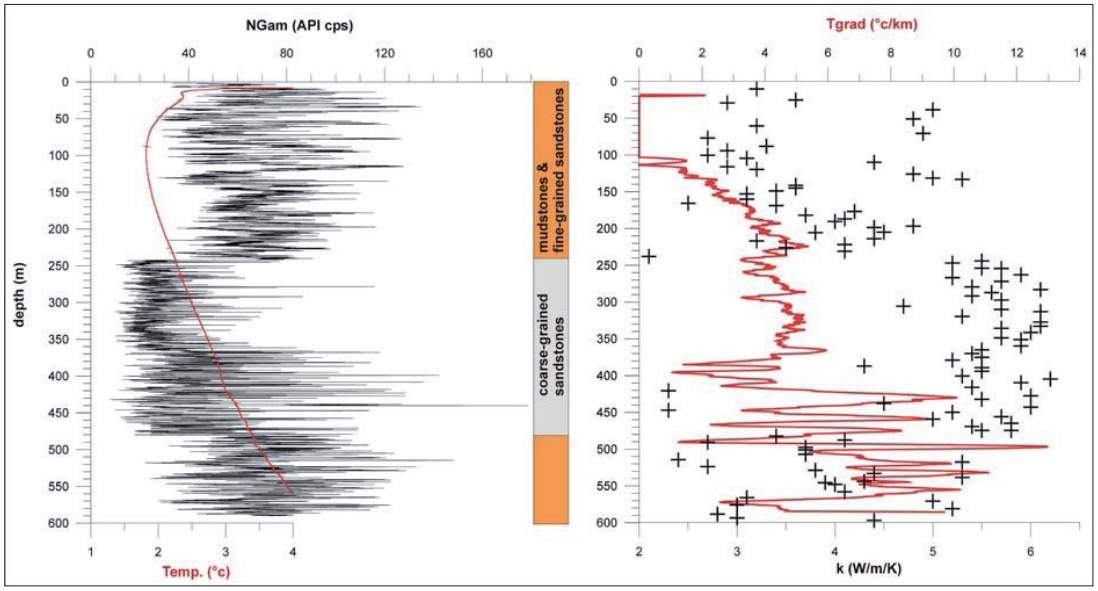

Figure 6. Left: *Gamma log from the Båtsfjordfjellet borehole with superimposed temperature profile and simplified lithostratigraphic column.* Right: *Thermal conductivities as measured on the drillcore, with the computed thermal gradient. For details, see Chapter 3 in Pascal et al. (2010).*

again, the quartz content has had a decisive effect in causing locally increased conductivity values.

Regional context of the borehole geology

In this northern part of Varanger Peninsula, rocks below the level of the Tanahorn Nappe (part of the Middle Allochthon of Scandinavian Caledonide tectonostratigraphy) (Figure 1) are involved in minor, syn-metamorphic, imbricate thrusting and form part of the Lower Allochthon. In this regard, the thrust emplacement of older Båtsfjord Formation rocks upon the Sandsfjorden Formation, as recognised in the Båtsfjordfjellet borehole, is not unexpected. The presence of gouge along the contact, representing a comparatively brittle component of fault movement, does, however, suggest that the thrust-fault was later reactivated during a phase of extension. Episodes of normal, extensional fault movement of Late Palaeozoic to Mesozoic age are well known from adjacent offshore areas (Gabrielsen & Færseth 1989, Bugge et al. 1995, Samuelsberg et al. 2003) and are suspected to have occurred onshore (Herrevold et al. 2009) and in Varangerfjorden (Roberts et al. 2011). Thinner gouge zones recorded in other parts of the drillcore may also represent brittle faults.

The actual location of the borehole is in the lowermost of two imbricate thrust sheets, the upper one known as the Rákkočearru thrust sheet (Herrevold et al. 2009, Roberts 2009) (Figure 1). The lower tectonic unit is here informally named the *Máhkirčearru thrust sheet* (Figure 1), the basal contact of which passes into Syltefjorden and can be followed offshore on recent aeromagnetic data (Gernigon et al. 2007).

The spaced, crenulation-type cleavage noted in some of the thin-sections is quite likely to correspond to the one reported from the nearby Kongsfjord area, in the Kongsfjord Formation, and the subject of a ^{40}Ar–^{39}Ar dating investigation (Rice and Frank 2003). This cleavage post-dates the main schistosity (which developed before 470 Ma) and most of the thrusting, and yielded a plateau age of *c.* 443 Ma (Rice and Frank 2003). This age corresponds to the Ordovician–Silurian boundary, and has not been recorded previously in Finnmark. Rice and Frank (2003) considered this pulse of deformation to have occurred approximately midway between the main, Early Ordovician (Finnmarkian) phase and the late-Caledonian, Siluro–Devonian (Scandian) event.

Conclusions

Logging of over 800 metres of drillcore from a borehole on Båtsfjordfjellet, Varanger Peninsula, revealed a succession of very low-grade, metasedimentary rocks which are assigned to two, specific, Neoproterozoic formations well known from regional mapping. The lowest c. 320 m of the core consist mostly of laminated maroon to greenish-grey mudstones, clay-rich rocks, thin sandstone beds and some dolomite ascribed to the Skovika Member of the Båtsfjord Formation. A weak spaced cleavage is seen in thin-sections of the mud- and clay-rich lithologies. This pelitic unit is overlain across an inferred unconformity by *c.* 230 m of coarse-grained sandstones with subordinate small-clast conglomerates, representing the Sandfjorden Formation of the Løkviksfjellet Group.

The upper *c.* 240 metres of the drillcore comprise a repetition of the Skovika Member mudrocks, with the basal contact against Sandfjorden sandstones marked by a thrust-fault that was later reactivated in a more brittle, and probably extensional regime.

Acknowledgements
Harald Elvebakk, NGU, carried out the logging of thermal conductivity and gamma-ray radiation. We thank him for his comments on these results and on an early version of the manuscript, and for allowing us to reproduce a figure (our Figure 6) from the Pascal et al. (2010) report. Cécile Barrère took photographs of the core at the time of logging, and Kirsti Midttømme is thanked for discussions of the geophysical results with the first author. Odleiv Olesen read and commented on the final manuscript, which was reviewed by Stephen Lippard. Irene Lundquist helped in preparation of the figures.

References

Bugge, T., Mangerud, G., Elvebakk, G., Mørk, A., Nilsson, I., Fanavoll, S. and Vigran, J.O. (1995) The Upper Palaeozoic succession on the Finnmark Platform, Barents Sea. *Norsk Geologisk Tidsskrift*, **75**, 3–30.

Gabrielsen, R.H. and Færseth, R.B. (1989) The inner shelf of North Cape, Norway and its implications for the Barents Shelf–Finnmark Caledonide boundary. A comment. *Norsk Geologisk Tidsskrift*, **69**, 57–62.

Gernigon, L., Marello, L., Moogaard, J.O., Werner, S.C. and Skilbrei, J.R. (2007) Barents Sea Aeromagnetic Survey BAS–06 – Acquisition, processing report and preliminary interpretation. *Norges geologiske undersøkelse Report 2007.035*, 144 pp.

Herrevold, T., Gabrielsen, R.H. and Roberts, D. (2009) Structural geology of the southeastern part of the Trollfjorden–Komagelva Fault Zone, Varanger Peninsula, Finnmark, North Norway. *Norwegian Journal of Geology*, **89**, 305–325.

Pascal, C., Barrère, C., Davidsen, B., Ebbing, J., Elvebakk, H., Gernigon, L., Olesen, O., Roberts, D., Siedlecka, A., Skilbrei, J.R., Slagstad, T. and Wissing, B. (2008) HeatBar Report 2008, Basement heat generation and heat flow in the western Barents Sea – importance for hydrocarbon systems. *Norges geologiske undersøkelse Report 2008.072*, 64 pp.

Pascal, C., Balling, N., Barrère, C., Davidsen, B., Ebbing, J., Elvebakk, H., Mesli, M., Roberts, D., Slagstad, T. and Willimoes-Wissing, B. (2010) HeatBar Final Report 2010, Basement Heat Generation and Heat Flow in the western Barents Sea – importance for hydrocarbon systems. *Norges geologiske undersøkelse Report 2010.030*, 91 pp.

Rice, A.H.N., Bevins, R.E., Robinson, D. and Roberts, D. (1989) Evolution of low-grade metamorphic zones in the Caledonides of Finnmark, N. Norway. *In:* Gayer, R.A. (ed.) *The Caledonide geology of Scandinavia*, Graham and Trotman, London, pp. 177–191.

Rice, A.H.N. and Frank, W. (2003) The early Caledonian (Finnmarkian) event reassessed in Finnmark: 40Ar/39Ar cleavage age data from NW Varangerhalvøya, N. Norway. *Tectonophysics*, **374**, 219–236.

Roberts, D. (2009) Berggrunnskart BERLEVÅG 2336–1, 1:50 000, revidert foreløpig utgave. *Norges geologiske undersøkelse*.

Roberts, D., Chand, S. and Rise, L. (2011) A half-graben of inferred Late Palaeozoic age in outer Varangerfjorden, Finnmark: evidence from seismic-reflection profiles and multibeam bathymetry. *Norwegian Journal of Geology*, **91**, 191–200.

Samuelsberg, T.J., Elvebakk, G. and Stemmerik, L. (2003) Late Palaeozoic evolution of the Finnmark Platform, southern Norwegian Barents Sea. *Norwegian Journal of Geology*, **83**, 351–362.

Siedlecka, A. and Roberts, D. (1992) The bedrock geology of Varanger Peninsula, Finnmark, North Norway: An excursion guide. *Norges geologiske undersøkelse Special Publication*, **5**, 45 pp.

Siedlecki, S. and Levell, B.K. (1978) Lithostratigraphy of the Late Precambrian Løkvikfjell Group on Varanger Peninsula, East Finnmark, North Norway. *Norges geologiske undersøkelse*, **343**, 73–85.

Addendum

Based on a recent reconsideration of the age of the Løkviksfjellet Group, this lithostratigraphic unit is now regarded as most likely Cryogenian (see the companion paper by Roberts and Siedlecka in this same Bulletin volume).

Appendix 1

DETAILED LOG OF THE BÅTSFJORDFJELLET DRILLCORE

Metres, from/to	Rock description	Sample no.	Box no.
2.20	Mudstone, greenish-grey and maroon, with crinkled lamination, in places disrupted. Possible desiccation cracks present. Dip c. 60º at 4.15 m.		B1 3 m
<4.95 4.95-7.80 7.80-9.35	Maroon mudstone. Very fine-grained sandstone, pinkish-grey, laminated, partly with carbonate cement. Ditto, grading downwards into thin carbonate beds and laminae, with interbeds of claystone.		B2
Up to c. 11.50	Mudstone, grey-green, interbedded with yellowish-grey carbonate rock (dolomite?). Uneven and disrupted lamination. Dip c. 60°.	BA001 10.35-10.45	B3
11.50-12.55 12.55-13.00 13.00-13.40 13.40-14.30	Gradual transition into mudstone and fine-grained sandstone. Uneven, disrupted lamination. Dip 50°. Mudstone, maroon and grey with intraformational breccia. Interbedded fine-grained sandstone and mudstone. Maroon mudstone with subordinate thin beds of pelitic carbonate rock.		B3
14.30-15.50 15.50-19.05 19.05-19.55	Very fine-grained sandstone with minor, thin, pelitic carbonate and maroon mudstone. Dip 60°. Maroon mudstone with intercalations of fine-grained sandstone. Disrupted lamination and desiccation cracks present. Fine-grained sandstone, pinkish-grey with subordinate brecciated laminae of mudstone.		B4
19.55-21.05 21.15-21.90 21.90-24.00	Same as 19.05-19.55. Interlaminated maroon mudstone and grey, clayey mudstone. Dip 60°. Maroon claystone/mudstone with some intraformational brecciated layers.		B5
24.00-28.55	Same as 21.90-24.00 with an increasing number of sandy intervals.	BA002 c. 25.40	B6
28.55-29.10 29.10-30.80 30.80-33.55	Same as above. Maroon mudstone/claystone with intervals of microbreccia. Maroon, in part grey, fine-grained sandstone with intervals of maroon mudstone; interrupted lamination.	BA003 29.20-29.30	B7
33.55-35.50 35.50-39.50	Pink sandstone, mostly fine-grained, with mm-thin uneven and brecciated laminae of maroon and green-grey mudstone. A few <1 cm-thick laminae of carbonate are present. Mainly very fine-grained, pink-grey sandstone with laminae of maroon claystone which decrease		B8

	in number downwards. Mostly rubble.		
39.50-40.95 40.95-42.60	Same as above. Dip 60°. Very fine-grained sandstone, pink-grey with a few disrupted, mm-thin laminae of maroon claystone.	BA004 38.50-38.60	B9
42.60-47.15	Pinkish-grey, fine-grained, massive sandstone with scattered thin veins of quartz. Dip horizontal.		B10
47.15-52.50	Massive sandstone, pinkish-grey, fine-grained. Lamination ?horizontal.	BA005 (TS) 51.00-51.10	B11
52.50-53.40 53.40-56.40 56.40-57.10	Same as above. Dip 60°. Very fine-grained sandstone, pinkish-grey, with discontinuous muddy laminae. Dip 60°. Maroon mudstone/claystone with crinkled lamination and a few thin beds of sandstone.		B12
57.10-57.85 57.85-60.25 60.25-61.00 61.00-61.90	Same as above. Fine-grained, pink-grey sandstone with abundant but disrupted laminae of maroon mudstone. Greenish-grey, laminated, muddy sandstone, carbonate-cemented (dolomitic?) with a few laminae of dolomicrite. Dip c. 60°. Alternating, grey, fine-grained sandstone and maroon mudstone/claystone with subordinate carbonate beds. Dip c. 60°.	BA006 (TS) 60.55-60.65	B13
61.90-67.20	Pinkish-grey, fine-grained sandstone, massive to laminated, with laminae of maroon mudstone. Mud chips and a few calcite-filled cavities and veinlets also present. Dip c. 60°.		B14
67.20-71.90	Fine-grained sandstone, as above, mostly massive.	BA 007 70.75-70.85	B15
71.90-72.10 72.10-72.65 72.65-76.20 76.20-76.45	Sandstone, as above, massive. Maroon mudstone and grey sandstone, thin-laminated with abundant claystone fragments (intraformational breccia). Massive to poorly laminated pink-grey sandstone. Rubble of maroon and grey mudstone.		B16
76.45-78.80 78.80-79.70 79.70-81.50	Maroon mudstone/claystone, mostly massive. Grey sandstone with laminae of claystone and a few thin carbonate layers. Grey, fine-grained sandstone with laminae of dark-grey mudstone. Scattered 'spots' of a ferruginous carbonate mineral present.	BA008 77.00-77.10	B17
81.50-82.80 82-80-83.10 83.10-85.00 85.00-86.65	Massive sandstone. Rubble of maroon mudstone. Grey, fine-grained, laminated sandstone with green-grey or maroon laminae of mudstone. Fine-grained, grey sandstone with many disrupted laminae of mudstone, in places chaotic and microbrecciated. Dip 65°.		B18
86.65-88.85 88.85-89.70	As above; mostly maroon mudstone with disrupted and brecciated lamination. Grey-green, fine-grained sandstone with grey	BA009 88.30-88.40	B19

	mudstone laminae. Dolomicrite(?) in upper part.		
89.70-91.20	Fine-grained sandstone and mudstone with disrupted lamination. Carbonate cement. Dip 65°.		
91.20-92.10	Fine-grained sandstone, massive, with some thin laminae of mudstone. Dip 65°.		
92.20-92.40	As above.	BA010 (TS) 94.20-94.30	B20
92.40-96.85	Maroon mudstone/claystone with intercalations of grey-green claystone. Laminae disrupted and partly microbrecciated.		
96.85-97.20	Grey sandstone with subordinate laminae of maroon mudstone. Dip 60°.		
97.20-100.10	Grey sandstone and thin laminae of maroon mudstone and thin beds of dolomicrite. Some sandstone beds have a carbonate cement.	BA011 100.40-100.55	B21
100.10-100.70	Maroon mudstone with a few sandy laminae.		
100.70-101.05	Sandy dolomite(?), laminated, with specks of a rusty mineral.		
101.05-102.20	Fine-grained, sandstone, laminated, with carbonate cement.		
102.20-103.65	As above.	BA012 (TS) 104.55-104.65	B22
103.65-104.70	Maroon mudstone with subordinate beds of fine-grained sandstone. Dolomicrite(?) layers in the lowest c. 15 cm.		
104.70-105-35	Grey sandstone and maroon mudstone, interlaminated.		
105.35-107.40	Grey, fine-grained sandstone, mostly laminated; lowermost part massive. Dip 70°.		
107.40-109.10	Fine-grained sandstone, laminated to massive.	BA013 (TS) 109.95-110.05	B23
109.10-109.60	Maroon lam. mudstone with sandstone interbeds.		
109.60-112.20	Fine-grained grey sandstone, laminated to massive, lamination disrupted. Grading into mudstone in the lower parts.		
112.20-112.75	As above.	BA014 116.00-116.10	B24
112.75-117.35	Maroon mudstone with interbeds of grey sandstone, partly brecciated.		
117.35-117.60	Mudstone as above.	BA015(TS) 119.60-119.70	B25
117.60-120.10	Grey sandy mudstone and pale-grey, thin-bedded sandstone, with calcite-cemented cracks.		
120.10-122.15	Grey sandstone and thin laminae of dark-grey mudstone (+ ?dolomicrite). Dip 75º.		
122.15-127.10	Pale-grey to pink-grey, fine-grained sandstone with grey mudstone laminae. Carbonate cemented. Dip 70º.	BA016 126.05-126.15	B26
127.10-132.20	Grey, fine-grained sandstone, massive. Dip 50º.	BA017 126.05-.15	B27
132.20-137.00	Grey, fine-grained sandstone, massive to partly laminated. Dip 65º.	BA018 133.35-.45	B28
137.00-140.00	Same as above.	BA019 141.50-141.60	B29
140.00-142.10	Maroon mudstone with subordinate intervals of grey sandstone. Disrupted lamination. Sandstone		

	beds show channelling and some graded bedding.		
142.10-146.60	Mostly the same maroon mudstone as above. Dip 80º.	BA020 145.10-.15	B30
146.60-152.10	Same as above. Dip near vertical.	BA021 148.90-.00	B31
152.10-152.40	Mudstone, same as above.	BA022 153.00-153.10	B32
152.40-152.85	Grey sandstone, fine-grained.		
152.85-153.20	Maroon and pink-grey alternating mudstone, claystone and sandstone with disrupted laminae.		
153.20-154.20	As above but with more sandstone. Dip 70º.		
154.20-154.70	Rubble, gouge, probable brittle fault.		
154.70-155.30	Greenish-grey, fine-grained sandstone with disturbed muddy laminae; carbonate cement.		
155.30-157.55	Well laminated maroon mudstone and grey, fine-grained sandstone.		
157.55-159.30	Same as above.	BA023 (TS) 160.20-160.30	B33
159.30-159.90	Pale-grey and pink-grey sandstone with greenish-grey to maroon mudstone laminae.		
159.90-160.80	Mostly maroon mudstone with abundant clay laminae and intraformational breccia.		
160.80-161.20	Variegated greenish-grey and maroon mudstone. Interbeds of sandstone/mudstone with subordinate clay laminae and some dolomicrite. Dip 50º.		
161.20-162.50	Greenish-grey mudstone and fine-grained grey sandstone, poorly laminated.		
162.50-162.80	As above, but mostly rubble.	BA024 165.80-.90	B34
162.80-167.50	Greenish-grey claystone interbedded with pinkish-grey sandstone. Lamination uneven with diverse, soft-sediment deformation structures. Subordinate carbonate-rich bands (Dolomicrite?). Dip from 70º to vertical.		
167.50-172.50	As above. The borehole cuts through vertical strata. Soft-sediment deformation structures are very common.	BA025 169.00-169.10	B35
172.50-175.20	As above but with more sandstone. Disrupted bedding common. Dip 50-80º.	BA026 176.90-177.00	B36
175.20-176.00	Rubble.		
176.00-177.20	Fine-grained grey sandstone with interbeds of grey claystone. Dip 60º.		
177.20-179.25	Green-grey mudstone with a few disrupted thin beds or laminae of carbonate rock (dolomicrite?).	BA027 182.00-182.10	B37
179.25-181.00	Mostly variegated sandstone, carbonate-cemented.		
181.00-182.35	Maroon mudstone with disrupted layers of grey sandstone. Dip 70º.		
182.35-182.70	Maroon mudstone as above.	BA028 187.00-187.10	B38
182.70-187.50	Pinkish-grey, fine-grained sandstone, carbonate-cemented, with crinkled laminae of maroon claystone.		
187.50-191.65	As above, disrupted lamination common.	BA029 190.50-	B39
191.65-192.80	Interbedded maroon mudstone and fine-grained		

	grey sandstone. Disrupted lamination very common. Dip 70-80º.	190.60	
192.80-197.65	Same as above, in places more sandy. Dip 70º.	BA030 196.80-.90	B40
197.65-197.75 197.75-201.25	As above, but mostly rubble. Fine-grained, yellow-grey, laminated sandstone, greyer in colour lower down. Dip 60º.	BA031 198.60-198.70	B41
201.25-204.50 204.50-205.45	Rubble of yellow-grey to green-grey sandstone. Fine- to coarse-grained sandstone with some muddy intervals and slump structures.	BA032 (TS) 205.05-205.15	B42
205.45-208.40 208.40-208.60 208.60-209.55	Sandstone as above, pale-grey, with subordinate clay intervals. Upper 40 cm shows soft-sediment deformation structures. Dip 60-70º. Green-grey claystone, laminated, in part a rubble of yellow-grey to green-grey sandstone. Grey, fine-grained sandstone, laminated.	BA033 (TS) 205.65-205.75	B43
209.55-214.90 214.90-215.15 215.15-215.55	Laminated sandstone and mudstone, variegated, partly with carbonate cement. Lowermost 50 cm mostly maroon mudstone. Dip 70º. Yellow-grey sandstone with maroon clay laminae, limonitic. Laminated grey sandstone and maroon mudstone.	BA034 213.95-214.05	B44
215.55-216.30 216.30-219.00 219.00-219.30	Pink-grey to yellow-grey, medium-grained sandstone. Grey, fine-grained sandstone and mudstone, distinctly laminated, carbonate-cemented. Pinkish-grey, laminated, fine-grained sandstone, carbonate-cemented. Dip 50º.	BA035 (TS) 216.90-217.00	B45
219.30-224.60	Sandstone as above, in places distinctly laminated. Dip 50º.	BA036 221.85-.95	B46
224.60-227.95 227.95-229.45 229.45-229.80	Fine-grained, laminated sandstone with maroon mudstone laminae. Carbonate cement. Lamination disrupted in places. Dip 65-70º. Variegated, partly yellow, limonitic sandstone with uneven muddy laminae. Fine-grained sandstone.	BA037 226.00-226.10	B47
229.80-234.50	As above, mostly massive but laminated in places. From 230.00 to 231.05 the lamination is more distinct. Dip 60º.	BA038 231.05-231.15	B48
234.50-236.45 236.45-238.50 238.50-239.30 239.30-241.55	As above. Fine- to medium-grained sandstone, variegated to yellow (limonitic), porous. Grey mudstone with sandstone laminae. Dip 55º. As above, but with a rubbly, greenish-grey, clay gouge at the base. **F A U L T**	BA039 238.00-238.10	B49
241.55-244.40	Pink-grey sandstone, faintly laminated, medium-to coarse-grained; middle part mostly rubble.	BA040 (TS) 244.10-.20	B50
244.40-249.40	As above, medium- to coarse-grained sandstone with gritty intervals composed of diverse, rounded clasts.	BA041(TS) 247.00-247.15	B51

249.40-251.15 251.15-254.05	As above. Pale-grey gritty sandstone, massive, in part a polymict granule conglomerate with diverse rock fragments. Dip c. 35º.	BA042 (TS) 254.00-.10	B52
254.05-259.70	Pale-grey and pink, gritty, feldspathic sandstone and polymict granule conglomerate with pink, grey and white pebbles. Dip c. 35º.	BA043 254.45- 254.55	B53
259.70-265.10	As above. Dip 35º, but this may be foreset beds in a cross-bedded unit.	BA044 254.45-.55	B54
265.10-265.50 265.50-270.10	Rubble of sandstone, as described above. Sandstone, as in B53. A c. 5 cm shaly interval occurs at 266.50.	BA045 266.95- 267.05	B55
270.10-275.00	As above. Rubble at 272.00-272.30. Dip c. 35º.	BA046 271.90-.00	B56
275.00-280.00	Pinkish- and greenish-grey sandstone, quartz-cemented, cross-bedded, coarse-grained or gritty with beds of granule conglomerate. Poorly sorted.	BA047 (TS) 279.50- 279.60	B57
280.00-285.50	As described above. Dip c. 30º.	BA048 283.15-.25	B58
285.50-291.70	As described above. Dip uncertain, c. 25º. Rubble at 288.70-291.00	BA049 287.20-.30	B59
291.70-295.90	As above. A c. 10 cm muddy interval at 292.70 with pebbles up to 1.5 cm across. Dip c. 30º.	BA050 291.70-.80	B60
295.90-301.00	As described above, coarse-grained sandstone. Muddy interval at c. 299.50 with dip c. 25º.	BA051 297.30-.40	B61
301.00-306.50	As described above, but colour now greenish-grey to pale maroon. Dip c. 25º at a muddy interval.	BA052 305.70-.80	B62
306.50-312.00	As described above. Dip 25º at a muddy interbed.	BA053 310.15-.25	B63
312.00-317.50	Pink and grey cross-bedded sandstone as described above, with a conglomerate in the lower 0.8 m; pebble size ≤ 1 cm. Dip (foresets?) 25-30º.	BA054 313.00- 313.10	B64
317.50-322.40	Sandstone, pink-grey, in places greenish-grey, poorly sorted, coarse-grained to gritty and with a polymict granule conglomerate with distinct fragments of red jasper. Dip as above.	BA055 319.60-.70	B65
322.40-327.50	Sandstone and conglomerate as above, with two 10-15 cm-thick clay-rich intervals.	BA056 327.20-.30	B66
327.50-333.25	The same sandstone and conglomerate as above.	BA057 332.90-.00	B67
333.25-335.25 335.25-336.15 336.15-336.50 336.50-336.90 336.90-339.00	The same sandstone as above. Polymict conglomerate. Diverse clast types up to 2 cm in size, including red jasper. Poorly sorted. Sandstone as in box 65. Polymict conglomerate, matrix-supported. Sandstone as in box 65.	BA058 335.70- 335.80	B68
339.00-344.70	Sandstone, coarse-grained to gritty, poorly sorted, interbedded with a fine-grained polymict conglomerate, matrix-supported as in box 65.	BA059 341.40- 341.50	B69

344.70-350.15	Small-pebble conglomerate with sandy matrix, poorly sorted, interbedded with coarse-grained sandstone plus a few clasts up to 1.5 cm in size.	BA060 348.70-348.80	B70
350.15-351.15 351.15-354.70 354.70-355.60	Conglomerate with clasts of quartz and red jasper, etc., matrix-supported; matrix gritty. Coarse-grained sandstone with a few scattered pebbles and angular rock fragments. Polymict conglomerate, though mostly with subrounded pebbles of quartz, up to 4 cm in size.	BA061 351.15-351.25	B71
355.60-356.90 356.90-361.30	Oligomict conglomerate with quartz and a few ≤ 2 cm, jasper clasts. Quartz cement. Dip 25-30º. Sandstone, coarse-grained to gritty, and granule conglomerate with clasts of quartz and jasper. Mudstone interval at 358.90-.95.	BA062 359.70-359.80	B72
361.30-361.90 361.90-366.00 366.00-367.15	Sandstone as above with scattered small pebbles. Oligomict conglomerate with subrounded to rounded pebbles mostly of quartz, up to 4 cm in size, and a little jasper. Dip 40º. Coarse-grained sandstone with scattered granule-size clasts, poorly sorted. One minor interval of maroon mudstone.	BA063 365.05-365.15	B73
367.15-371.40	Coarse-grained, grey sandstone with sporadic small pebbles and a few <3 cm interbeds of maroon mudstone. Dip 30º.	BA064 370.00-.10	B74
371.40-376.60	Medium- to coarse-grained sandstone with a few <2 cm intercalations of claystone which have acted as slip planes. Rare small clasts at some levels, and a few quartz veins. Dip 30º.	BA065 375.10-375.20	B75
376.60-380.95 380.95-381.25 381.25-381.40	As above, coarse-grained sandstone, with a few scattered pebbles up to 1.5 cm in size. Maroon to green-grey mudstone with a few clasts. Coarse sandstone with a few small pebbles.	BA066 379.05-379.15	B76
381.40-387.20	Sandstone, pink-grey, medium- to coarse-grained, poorly sorted. Quartz cemented. Intervals of maroon mudstone 3-10 cm thick at 381.55, 383.40 and 383.70.	BA067 387.00-.10	B77
387.20-392.40	Sandstone as above, with one interval of greenish-grey fine-grained sandstone at 390.20-390.45. Tectonic disturbance at this level (*two photos*).	BA068 389.25-389.35	B78
392.40-397.10	Sandstone, fine- to coarse-grained, partly gritty, quartz cement, moderately/poorly sorted. Dip 30º.	BA069 340.00-.10	B79
397.10-402.80	As above, coarse-grained sandstone.	BA070 400.50-.60	B80
402.80-407.40	Sandstone, grey, coarse-grained to gritty, quartz-cemented, with a few granule-size rock fragments.	BA071 404.75-.85	B81
407.40-412.55	As above, but with some 3-6 cm-thick intervals of finer grained sandstone.	BA072 409.70-.80	B82
412.55-418.00	As above, very little variation. Dip c. 25º.	BA073 416.05-.15	B83

418.00-420.50 420.50-420-85 420.85-423.35	Sandstone. Medium- to coarse-grained, partly gritty, some <0.5 cm clasts. Quartz-cemented. Sandstone, dark-grey, fine-grained. Some very small-scale cross bedding. Partly rubble. Sandstone, medium- to coarse-grained, or gritty, a few clasts <0.5 cm. Quartz-cemented. A fine-grained interval at the base of the core in this box.	BA074 420.65- 420.75	B84
423.35-426.40 426.40-426.55 426.55-428.00	Sandstone, as above. Fine-grained muddy sandstone with near-vertical cleavage. Sandstone, medium- to coarse-grained, feldspathic, quartz-cemented.	BA075 427.65- 427.75	B85
428.00-433.25	Sandstone, as above, mostly coarse-grained, with two <3 cm beds of grey mudstone. Dip 25-30º.	BA076 432.20-.30	B86
433.25-434.00 434.00-434.10 434.10-435.10 435.10-436.70 436.70-438.10 438.10-438.20	As above. Fine-grained muddy sandstone with vertical cleavage. Coarse-grained sandstone, tectonically brecciated. Rubble of sandstone. Medium- to coarse-grained sandstone, quartz cemented. Fine-grained sandstone (see box 88)	BA077 437.90- 438.10	B87
438.20-440.50 440.50-443.40	Green-grey, fine-grained, muddy sandstone, unevenly laminated with subordinate, coarse-grained intervals. Sandstone, medium- to coarse-grained, quartz-cemented, feldspathic, partly a grit or granule conglomerate. Dip 30º.	BA078 443.05- 443.15	B88
443.40-446.60 446.60-447.40 447.40-448.30	As above, mostly coarse-grained. Dip 35º. Sandstone, dark-grey, fine-grained, massive to faintly laminated. Medium-grained, grey sandstone.	BA079 447.10- 447.20	BA89
448.30-449.30 449.30-453.15 453.15-453.80	As above. Coarse-grained sandstone with many ≤7 cm clasts of mudstone arising from intraformational erosion. Much granule-size material lower down. Sandstone, med.- to coarse-grained, see box 91.	BA080 449.80- 450.00	B90
453.80-455.40 455.40-456.00 456.00-457.80	As above, coarse-grained. Dip 40º. Rubble of sandstone. Medium- to coarse-grained grey sandstone. One 20 cm interval of dark-grey, laminated, muddy sandstone.	BA081 456.15- 456.25	B91
457.80-458.10 458.10-458.25 458.25-458.45 458.45-458.60 458.60-462.60	As above. Sandstone, greenish-grey, muddy, fine-grained. Rubble of pink, medium-grained sandstone. Rubble of claystone. Mostly coarse-grained sandstone with clasts of intraformational claystone. Dip 35º.	BA082 459.20- 459.30	B92
462.60-467.50	Feldspathic sandstone, medium- to very coarse-grained (gritty), quartz-cemented, with small	BA083 464.85-	B93

	clasts of mudstone. Dip 40º.	464.95	
467.50-472.40	Grey sandstone, fine- to coarse-grained, with a few, sharp, erosional bases to individual beds. Intercalations of a darker grey, laminated, muddy sandstone. 471.00-471.50 mostly rubble. Dip 35º.	BA084 469.20-469.30	B94
472.40-477.50	Grey sandstone, medium- to coarse-grained with sporadic subangular clasts (≤3 cm) of very fine-grained sandstone. Dip 35º. A 10 cm bed of calcareous claystone (rubbly) at c. 476.00, and a muddy layer with calcite along bedding at 477.25.	BA085 474.65-474.75	B95
477.50-479.15 479.15-481-30 481.30-482.80	Grey sandstone, medium-grained, finer grained lower down. Cross-bedding in uppermost metre with clasts of mudstone. Very coarse-grained sandstone, feldspathic, with subangular to subrounded fragments of mudstone 3 cm in size. **REGIONAL UNCONFORMITY** Mudstone, in part sandstone, grey to dark-grey, thin-bedded/laminated with many soft-sediment deformation structures. Dip 30º.	BA086 (TS) 482.20-482.30	B96
482.80-488.50	Grey, fine-grained sandstone, dolomitic, massive to weakly laminated, interbedded with a laminated dolomitic mudstone with soft-sediment deformation structures. Dip 30º.	BA087 (TS) 487.80-487.90	B97
488.50-493.55	As above, with white carbonate interbeds (dolomicrite?) up to 2 cm thick. At 491 m, colour changes to variegated, in part maroon (mudstone).	BA088 (TS) 490-70-490-80	B98
493.55-499.70	Interbedded laminated maroon mudstone and grey, fine-grained sandstone. Lamination disrupted with a few small-scale faults (some may be synsedimentary). Dip 20-25º.	BA089 497.50-497.60	B99
499.70-504.10	Interbedded fine-grained, laminated, grey sandstone and maroon mudstone, as above.	BA090 501.00-.10	B100
504.10-509.60	As above, but here with an increasing volume of laminated maroon mudstone. Dip 30º.	BA091 507.00-.10	B101
509.60-514.80	As above, maroon mudstone and grey sandstone. Calcareous bed (2 cm) at 514.50. Dip 25-30º.	BA092 510.40-.50	B102
514.80-518.80 518.80-520.25	As above, but with pink-grey laminated sandstone in the lowest 2.5 m. Partly calcareous. Rubble of fine-grained muddy sandstone.	BA093 517.70-517.80	B103
520.25-521.50 521.50-524.80	Sandstone, fine-grained, massive, calcareous. Laminated grey sandstone and maroon mudstone. Some small-scale cross-bedding in the sandstone. Lamination strongly disturbed. Dip 30º.	BA094 523.85-523.95	B104
524.80-530.00	Predominantly laminated maroon mudstone. Subordinate sandstone intervals.	BA095 528.80-.90	B105
530.00-532.80	Interbedded variegated, pink-grey, fine-grained sandstone and maroon mudstone/claystone. Subordinate dolomicrite laminae and pink calcite veins. Deformed lamination in the lower 0.5 m.	BA096 533.10-533.20	B106

532.80-535.50	Pinkish-grey, fine-grained sandstone, slightly calcareous, weakly laminated to massive. Dip 20º.		
535.50-540.90	As above, pink-grey sandstone with one unit of maroon mudstone in the upper part. Dip 25º.	BA097 538.65-538.75	B107
540.90-541.30	Maroon mudstone.		
541.30-541.40	Pinkish-grey, fine-grained sandstone.		
541.40-545.65	Interbedded maroon mudstone and green-grey, fine-grained sand/siltstone, partly massive.	BA098 545.75-545.85	B108
545.65-546.10	Sandstone, grey, laminated, fine-grained.		
546.10-546.70	Sandstone, as above, mostly coarse-grained.	BA099 548.00-548.10	B109
546.70-550.80	Variegated fine-grained sandstone/mudstone with disrupted maroon mudstone laminae.		
550.80-551.40	Grey, fine-grained sandstone, lam. to massive.		
551.40-551.70	Maroon mudstone.		
551.70-554.90	Interbedded maroon mudstone and variegated, fine-grained sandstone with disrupted mudstone laminae. Dip 20-25º.	BA100 554.00-554.10	B110
554.90-555.10	Greenish-grey calcareous mudstone with subordinate laminae of dolomicrite.		
555.10-556.80	Grey, laminated to massive sandstone, partly calcareous.		
556.80-557.20	Interbedded maroon mudstone and sandstone.		
557.20-557.25	Mudstone as above.	BA101 558.10-558.20	B111
557.25-557.85	Interbedded grey mudstone and fine-grained sandstone, some dolomicrite laminae; also slump structures.		
557.85-559.50	Pink-grey sandstone, weakly lam., calcareous. Erosional contact at base with clay chips.		
559.50-562.60	Variegated, laminated, grey, fine-grained sandstone and mudstone. (*see photo of slump structures in the uppermost part of this box*)		
562.60-564.30	Fine-grained laminated, calcareous sandstone and maroon mudstone.	BA102 566.00-566.10	B112
564.30-566.10	Maroon lam. mudstone, with synaeresis cracks.		
566.10-566.60	Interlaminated, fine-grained sandstone and maroon mudstone.		
566.60-566.80	Grey, laminated mudstone with dolomicrite laminae. Upper contact sharp, tectonised.		
566.80-568.00	Laminated, grey, fine-grained calc-sandstone.		
568.00-572.90	Sandstone, as described above. About 50% of the drillcore is rubble.	BA103 570.80-.90	B113
572.90-573.80	As above, partly rubble.	BA104 575.90-576.00	B114
573.80-578.10	Interbedded, variegated mudstone and fine-grained sandstone, with disrupted laminae of claystone. Intervals with soft-sediment deformation structures. Some calcite veins.		
578.10-583.50	Variegated, lam. sandstone and maroon mudstone. Laminae disrupted. A more massive, fine-grained sandstone bed at c. 581.10-581.70. Dip 35-40º.	BA105 581.10-.20	B115
583.50-583.75	Variegated laminated mudstone and subordinate	BA106	B116

	dolomicrite. Disrupted lamination.	588.50-588.60	
583.75-586.60	As above, with fine-grained sandstone, calcareous.		
586.60-586.90	Laminated, green-grey mudstone, claystone and dolomicrite.		
586.90-588.00	Fine-grained sandstone, unevenly bedded.		
588.00-588.60	Laminated sandstone and dark-grey mudstone.		
588.60-589.20	As above, with transition downwards to	BA107 (TS) 593.50-593.60	B117
589.20-590.90	Grey sandstone with darker claystone interbeds.		
590.90-592.70	Laminated green-grey sandstone and subordinate mudstone and dolomicrite; massive at 591.75-.95.		
592.70-593.40	Variegated mudstone and sandstone.		
593.40-593.85	Grey, laminated, dolomitic claystone, fine-grained sandstone and clayey dolomicrite.		
593.85-594.05	Grey, laminated, fine-grained sandstone.		
594.05-598.10	As above, laminated, with some maroon mudstone in the middle part. Dip 30º.	BA108 596.90-597.00	B118
598.10-598.50	Maroon, massive to laminated mudstone with thin sandstone beds in the lower part (partly rubble).		
598.50-599.30	Sandstone, fine-grained, grey, massive to weakly laminated, calcareous.		
599.30-604.25	Sandstone, pinkish-grey, massive, poorly laminated.	BA109 603.25-.35	B119
604.25-609.05	As above. Tectonised zone at 607.20-607.40 consisting of a friable gouge. This is a possible brittle fault. Dip c. 15º.	BA110 605.35-.45	B120
609.05-614.40	As above, with a few laminae and a 1 cm interval of maroon mudstone in the middle part. Dip 30º.	BA111 609.35-.45	B121
614.40-614.60	Sandstone as above.	BA112 618.35-618.45	B122
614.60-615.30	Grey and maroon mudstone, strongly tectonised (breccias and some gouge). Possible fault.		
615.30-615.55	Thin-bedded sandstone and maroon mudstone.		
615.55-615.80	Interbedded grey mudstone and grey dolomicrite.		
615.80-616.85	Laminated pale-grey sandstone with subordinate muddy maroon laminae.		
616.85-618.70	Greenish-grey lam. dolomicrite and mudstone.		
618.70-619.00	Sandstone, laminated, dip 45º.		
619.00-619.90	Maroon mudstone with a few sandy laminae and with soft-sediment deformation structures.		
619.90-630 ?	*Impossible to log correctly boxes 123 & 124 because of missing core (only 40% present) and incorrect or confusing depth numbering. The boxes contain pink-grey, fine-grained sandstone with maroon/grey mudstone and dolomicrite.*	BA113	B123 & B124
630.00-635.05	Pinkish-grey, fine-grained, laminated sandstone with scattered chips of maroon mudstone. Dip 30º. *(OBS: broken box, some drillcore missing).*	BA114 633.05-633.15	B125
635.05-635.40	Sandstone, as above.	BA115 (TS) 636.05-636.15	B126
635.40-636.30	Interbedded green-grey, laminated mudstone, fine-grained sandstone and dolomicrite. Upper part tectonised.		

636.30-640.50	Pink-grey, fine-grained, laminated and in part massive sandstone, weakly calcareous.		
640.50-643.45	As above, lowest 15 cm geen-grey, laminated mudstone and weakly calcareous sandstone. 15 cm of maroon mudstone at and below 641.50.	BA116 643.50-643.60	B127
643.45-643.80	Maroon mudstone, some slumping in lower part.		
643.80-644.05	Sandstone as in the highest part of this box.		
644.05-644.45	Maroon mudstone.		
644.45-645.00	Sandstone, as above. Dip 40º.		
645.00-651.50	Sandstone, as above, with a few mudstone chips. Mudstone layers at 650.00-.20 and 648.60-650.00.	BA117 650.05-.15	B128
651.50-656.50	Sandstone, pinkish-grey as above with subordinate Intervals of maroon mudstone.	BA118 656.40-.50	B129
656.50-656.85	Maroon mudstone.	BA119 660.10-660.20	B130
656.85-660.10	Pink-grey sandstone, massive, partly laminated, with a few mud chips. A variegated interval with dolomicrite laminae at 657.30-657.50.		
660.10-660.90	Laminated maroon mudstone, partly disrupted.		
660.90-662.30	Pinkish-grey, laminated sandstone.		
662.30-668.00	Pink-grey, fine-grained sandstone, massive to faintly laminated with two beds of mudstone. At 667.20, gradual transition downwards into lam. maroon mudstone with disrupted laminae.	BA120 666.70-666.80	B131
668.00-668.20	As above, mudstone.	BA121 671.10-671.20	B132
668.20-673.50	Pink-grey, fine-grained sandstone, massive to laminated with some chips and laminae of maroon mudstone. A few quartz veins in lowest 2 m.		
673.50-676.20	Sandstone, as above, with many quartz veins.	BA122 674.35-674.45	B133
676.20-676.35	Maroon mudstone. Dip 25º.		
676-35-676.50	Pink-grey sandstone. (*Only 50% of the core in strip 4. No core at all in strip 5.)*		
678.45-679.00	Laminated maroon mudstone.		
679.00-679.40	Mudstone, as above.	BA123 679.90-680.00	B134
679.40-682.00	Sandstone, grey, with subordinate intercalations of laminated mudstone. Dip 20-25º.		
682.00-683.50	Laminated maroon mudstone.		
683.50-684.00	Grey sandstone, weakly laminated.		
684.00-684.30	Pinkish-grey sandstone.	BA124 689.90-690.00	B135
684.30-686.20	Laminated fine-grained sandstone, with mudstone at 685.10-686.40 and 685.90-686.00. Dip 30º.		
686.20-687.00	Maroon mudstone with sandstone beds up to 6 cm thick. Abundant soft-sed. deformation structures.		
687.00-688.00	Pink-grey, fine-grained sandstone.		
688.00-689.00	Laminated maroon mudstone.		
689.00-690.50	Sandstone, as above.		
690.50-692.15	Pink-grey, weakly laminated sandstone with mudstone chips in some beds. Dip 30º.	BA125 694.90-695.00	B136
692.15-693.50	Maroon laminated mudstone with disrupted laminae. Some <10 cm-thick sandstone interbeds.		
693.50-696.00	Mostly pink-grey, fine-grained, laminated		

	sandstone with a few quartz and calcite veins, and two subordinate, <15 cm, mudstone intervals.		
696.00-697.00 607.00-699.00 700.50-701.25	Maroon mudstone with some greyish-maroon, fine-grained sandstone. Greenish-grey laminated mudstone and grey fine-grained sandstone and some dolomicrite. Soft-sed. deformation structures common. 15 cm bed of reddish sandstone. (*Obs! 1.5 m of core missing)* Greenish-grey sandstone and mudstone with a few laminae of dolomicrite.	BA126 (TS) 698.75-698.85	B137
701.25-707.10	As above. Soft-sediment deformation structures are abundant. One maroon-grey unit at 704.40-704.70, otherwise grey sandstone and mudstone.	BA127 704.50-704.60	B138
707.10-712.00 712.00-712.60	As above, but a bit coarser-grained and well lam. lower down. Abundant soft-sed. deformation structures, also with water-escape structures and synaeresis cracks. Transition down into maroon mudstone.	BA128 707.45-707.55	B139
712.60-712.75 712.75-713.65 713.65-714.10 714.10-717.70	As above. Sandstone, pink-grey, massive to weakly lam. with quartz and calcite veins. Lower 25 cm mudst. Variegated, calc., fine/medium-gr. sandstone. Alternating grey/pink-grey sandstone and maroon mudstone, with chips of mudst. in the sandstone.	BA129 717.40-717.50	B140
717.70-719.05 719.05-719.60 719.60-719.95 719.95-720.90 720.90-723.60	Pink-grey sandstone, fine-grained, calcareous, in places with many tiny chips of maroon mudstone. Laminated maroon mudstone. Dip 30º. Pinkish-grey sandstone. Laminated maroon mudstone. Grey or pink-grey to maroon, lam., fine-grained sandstone, calcareous, with veins of quartz/calcite.	BA130 722.00-722.10	B141
723.60-725.90 725.90-726.45 726.45-727.60 727.60-729.00	Pink-grey sandstone, massive to laminated, partly calcareous with calcite and quartz veins. Grey to maroon mudstone and sandstone. Fault with dip 70º, brecciated. Dip of bedding 25-40º. Grey to pink-grey sandstone, uneven lamination. Maroon lam. mudstone with some sandy intervals.	BA131 724.90-725.00	B142
729.00-729.10 729.10-731.40 731.40-731.60 731.60-734.50	As above. Fine-grained sandstone with some maroon muddy laminae. Wavy lamination in middle part, mudstone fragments in lowermost part. Rubble of disrupted/tectonised mudstone. Grey, laminated sandstone, in part calcareous, rich in quartz and calcite veins.	BA132 733.70-733.80	B143
734.50-735.30 735.30-736.50 736.50-737.70 737.70-738.75 738.75-740.00	As above. Maroon mudstone, weakly laminated. Grey, fine-gr. sandstone, partly calcareous. Laminated, greenish-grey mudstone and dolomicrite with soft-sed. deformation structures. Grey sandstone, calcareous, unevenly laminated.	BA133 736.85-736.95	B144

740.00-741.80 741.80-742.70 742.70-745.20	Grey sandstone and maroon mudstone with wavy and disrupted laminae. Variegated to green-grey sandstone with some dolomicrite laminae. Pink-grey sandstone and maroon lam. mudstone with soft-sed. deformation structures. Dip 25º.	BA134 742.55- 742.65	B145
745.20-747.15 747.15-750.80	Maroon laminated mudstone with subordinate sandy intervals, e.g. at 745.80-745.95. Pale-grey to green-grey, fine-grained sandstone and mudstone, calcareous, ?dolomicrite laminae. Cavity filings of calcite in middle part. Dip 30º.	BA135 749.85- 749.95	B146
750.80-751.20 751.20-754.75 754.75-756.35	As above. Maroon lam. mudstone, a few sandy laminae. Pink-grey, fine-grained sandstone, laminated, in places with fragments of maroon mudstone.	BA136 753.95- 754.05	B147
756.35-760.20 760.20-761.60	Fine-grained sandstone, massive to laminated, slightly calcareous; veins of quartz and calcite. Variegated fine-grained sandstone and mudstone, lamination wavy and disrupted; calcareous.	BA137 761.30- 761.40	B148
761.60-762.10 762.10-764.70 764.70-766.05 766.05-766.90	As above. Maroon mudstone with wavy or disrupted lamination, a few thin beds of sandstone. Dip 20º. Transition into grey sandstone and maroon mudstone with soft-sed. deformation structures. Slightly calcareous. Sharp basal erosional contact. Mostly maroon laminated mudstone.	BA138 764.65- 764.75	B149
766.90-769.40 769.40-772.55	Mudst. as above. Sandstone bed at 767.00-767.15. Green-grey, fine-grained sandstone and mudstone with abundant soft-sed. deformation structures. Some possible dolomicrite laminae.	BA139 770.75- 770.85	B150
772.55-774.30 774.30-776.50 776.50-777.50	As above, but mostly rubble. Maroon mudstone, but poorly laminated. Grey sandstone, brittle and porous. Lower part mostly rubble.	BA140 776.75- 776.85	B151
777.50-779.60 779.60-781.20 781.20-782.10	As above, first 2 m mostly rubble. Fine-grained sandstone, laminated in the lowermost 50 cm. Transition into maroon mudstone, massive to laminated, with disrupted laminae. Gradual transition downwards into pale green-grey, lam. sandstone and mudstone, with some thin dolomicrite beds. Many soft-sed. deformation structures, including water escape structures.	BA141 779.30- 779.40	B152
782.10-786.00 786.00-787.35	As above, well laminated to massive, in part with chaotic soft-sed. deformation structures. Dip 30º. Maroon to grey-maroon mudstone to fine-grained muddy sandstone with many tiny chips of clay.	BA142 782.45- 782.55	B153
787.25-788.55 788.55-790.50	Maroon mudstone, poorly laminated, with some fine-grained, laminated sandstone in lower 40 cm. Fine-grained grey sandstone with laminae of maroon and grey mudstone, and possibly	BA143 791.60- 791.70	B154

	dolomicrite. Some sstn beds are calcareous.		
790.50-791.00	Maroon mudstone with some sandstone laminae.		
791.00-793.00	Variegated, fine-grained sandstone and mudstone, uneven lamination, soft-sediment deformation structures present, partly calcareous.		
793.00-794.00	Distinctly laminated, dark-grey mudstone and pale-grey, fine-grained sandstone. Soft-sediment deformation structures present.	BA144 794.55-794.65	B155
794.00-797.90	Grey, fine-grained sandstone and greenish-grey mudstone; wavy/disrupted lamination. Dip 20º.		
797.90-798.00	Maroon mudstone, poorly laminated. Chaotic soft-sediment deformation structures lower down.		
798.00-800.15	Mudstone, as above.	BA145 800.25-800.35	B156
800.15-801.35	Greenish-grey and pink-grey sandstone with interbeds of green-grey mudstone. Laminae disrupted, some possibly calcareous. *OBS! - The last c. 1 metre of core is fractured and rubbly. The exact base of the core is unknown.*		

Appendix 2

Heat Bar drillcore, Båtsfjordfjellet: brief descriptions of thin-sections of rocks from the core

Eighteen thin-sections have been examined with the main focus on the following objectives:

1. Mineral composition.
2. Textures (primarily grain size and sorting) and microstructure.
3. Correlation of the results of (1) and (2) with the measurements of thermal conductivity.

Brief descriptions of the thin-sections (downwards in the core).

For precise locations of the core samples taken for thin-sections (numbers BA 005 to BA 126) from the drillcore, see Appendix 1.

Båtsfjord Formation, Skovika Member

BA 005 Fine-grained (c. 0.1 - 0.2 mm), well-sorted quartz sandstone composed of subangular to subrounded grains of quartz and some feldspar. Sericite is the main component of the cement, which also contains some tiny grains of red jasper and hematite dust. Several of the quartz grains have clearly visible quartz overgrowths, whilst dentate contacts between some other quartz grains suggest the presence of overgrowths but with no visible boundary between the clastic grain and the authigenic overgrowth.

BA 006 (a) Very fine-grained quartz sandstone and siltstone (c. 0.05 - 0.1 mm), moderately sorted, grains subangular. Subordinate feldspar. Cement: carbonate (dolomite). Specks of an opaque, Fe-oxide mineral common, (b) dolomicrite laminae with sporadic chlorite flakes. Features indicative of compaction can be seen in some layers.

BA 010 Hematite-rich mudstone with scattered sand-sized grains of quartz, angular to subrounded. There are also sand-sized fragments of disrupted (dolo)micritic laminae. Subordinate feldspar.

BA 012 Hematite-rich mudstone (0.05 - 0.1 mm) with very fine sand + silt, subangular, with some c. 0.2 mm grains = fine sand. The hematite-rich laminae alternate with sericite laminae containing little or no hematite. Subordinate feldspar grains. A compactional fabric can be detected in some layers (laminae folia flattened around quartz-rich lenses).

BA 015 Alternating laminae of dolomicrite and laminae consisting of very fine sand- and silt-sized quartz grains (0.04 – 0.1 mm), subangular to angular, in

an abundant carbonate + sericite cement. Traces of a spaced cleavage oriented at c. 10-15° to the lamination can be seen in some layers.

BA 023 Laminated sandy mudstone, 0.05 - 0.35 mm = silt, with medium-grained quartz sand grains, subangular to subrounded, rich in (authigenic) hematite. Subordinate feldspar, rare (classic) chlorite. Cement: dolomite forming c. 0.05 mm rhombohedra. Clayey laminae consist of sericite and hematite. A weak spaced cleavage is present in some layers.

BA 033 (a) Fine-grained (0.15 - 0.2 mm) well-sorted, grain-supported feldspathic sandstone, sericite-cemented. Some chlorite and (Fe) sulphide concentrations. Sporadic c. 0.5 mm sand grains (wind blown).
(b) Mudstone, clay (sericite)-rich with subangular to subrounded quartz grains. Scattered subrounded quartz grains c. 0.6 - 1 mm (coarse to very coarse, interpreted as wind blown). Faint spaced cleavage and grain orientation at c. 10° to layering.

BA 035 Dolomicrite (<0.01 - 0.02 mm), homogeneous, with some c. 1 mm-thick laminae of quartz siltstone (≤ 0.05 mm) and very fine-grained sandstone. Subordinate laminae of quartz silt+sericite. Voids and cracks are sealed with carbonate. Subordinate feldspar, chlorite and opaque minerals (?FeS) in small scattered concentrations (spots). Weak spaced cleavage detectable.

(fault contact)

Løkviksfjellet Group, Sandfjorden Formation

BA 040 Quartz sandstone, grain-supported, coarse- to very coarse-grained (c. 0.5 - 1.3 mm), grains rounded to well-rounded; subordinate grains of feldspar, chert and quartzite. The majority of the quartz grains are markedly strained. The quartzite grains are tightly packed, and there are some intergranular pockets filled with fine grains of quartz. Quartz overgrowths are discernible in only a few places. Thin rims of sericite + ?chlorite cement.

BA 041 Quartz sandstone, grain-supported, coarse- to very coarse-grained (c. 0.4 - 1.0 mm) with some granules (2 - 4 mm). The quartz grains are rounded to well-rounded, and there are many strained grains. A few grains exhibit quartz overgrowths (probably the majority of overgrowth rims are not visible because of the clean surfaces of the clastic grains). Feldspar and chert grains are subordinate. Pockets of quartz silt and sericite (?clastic or ?crushed or ?weathered feldspar). The negligible cement consists of sericite and chlorite. One 5 mm quartz pebble is present in this thin-section.

BA 042 Quartz sandstone, grain-supported, very coarse-grained, gritty with granules. The grains are rounded to well-rounded and tightly packed. Some are strained. There are granules of quartzite, chert and red jasper. Also present are small intergranular pockets filled with equigranular quartz silt (?) = ?crushed larger grains or ?weathered feldspar.

BA 047 Quartz sandstone, coarse- to very coarse-grained, gritty, with granules and small pebbles of quartz, quartzite and chert. Large subrounded grains may be wind blown. There are distinct quartz overgrowths on several quartz grains, and dentate contacts between quartz grains are suggestive of overgrowths on clean surfaces of clastic grains. Pockets between the coarse grains are filled with 0.1 - 0.2 mm quartz sand. Feldspar grains are few and weathered. Thin (c. 0.02 mm) rims of cement consist of sericite and chlorite. Also present are some round opaque grains c. 0.1 - 0.3 mm in diameter.

(*unconformity)*

Båtsfjord Formation, Skovika Member:

BA 086 Laminated mudstone with lamination-parallel cracks and lenticular voids filled with dolomite, and several mm-thick veinlets of coarse dolomite. The mudstone shows a faintly developed cleavage oriented at c. 20° to the lamination. Quartz grains show nice dissolution features where they are in contact with cleavage folia, and beards or tails within the inter-cleavage domains.

BA 087 Laminated, dolomitic claystone/mudstone and muddy fine-crystalline dolomite. Synsedimentary voids and cracks are filled with dolomite and fibrous ?gypsum. Traces of a spaced cleavage can be seen in the finer-grained layers.

BA 088 Dolomicrite, laminated, with some laminae enriched in quartz sand and silt.Voids, cracks and minute pores are filled with fibrous (?)gypsum + dolomite + quartz. In places, the fibrous (?)gypsum appears to be replaced by carbonate (dolomite). Mud-enriched parts are poorly sorted and clearly enriched in hematite dust and tiny quartz grains. A faint spaced cleavage is present in some layers.

BA 107 Laminated, clayey (sericitic) dolomicrite (0.01 - 0.02 mm) and dolomitic claystone, and fine-grained (0.02 – 0.05 mm) dolomite. The laminae contain scattered quartz grains mostly <1 mm in size. A compactional fabric is detectable. Some small syn-sedimentary faults offset laminae at right-angles and then curve and die out along the layering.

BA 115 Laminated dolomicrite (< 0.01 mm) and dolomitic mudstone. Abundant cracks and voids in dolomicrite are filled with dolomite and (?)gypsum. A crude spaced cleavage is present in some finer-grained layers, and can also be detected in quartz-rich, carbonate-cemented layers.

BA 126 Laminated dolomicrite and dolomitic mudstone. Fractures c. 0.25 mm wide are sealed with a carbonate mineral. These veinlets transect the layering at 50-55°. They also cut across a weak spaced cleavage but are themselves displaced along these same cleavage surfaces.